System Reliability of Structural Steel Frames Designed Using Component- and System-Based Design Methods

Damir Akchurin[1, †], Sándor Ádány[2, 3], Ronald D. Ziemian[4], Kim J. R. Rasmussen[5], Benjamin W. Schafer[6]

[1]Graduate Research Assistant, Department of Civil and Systems Engineering, Johns Hopkins University, Baltimore, MD, USA

[2]Associate Research Scientist, Department of Civil and Systems Engineering, Johns Hopkins University, Baltimore, MD, USA

[3]Professor, Department of Structural Mechanics, Budapest University of Technology and Economics, Budapest Hungary

[4]Professor, Department of Civil and Environmental Engineering, Bucknell University, Lewisburg, PA, USA

[5]Professor, School of Civil Engineering, University of Sydney, Sydney, NSW, Australia

[6]Professor, Department of Civil and Systems Engineering, Johns Hopkins University, Baltimore, MD, USA

[†]Corresponding author, akchurd1@jhu.edu

Abstract

The current design practice for structural steel buildings is largely governed by component-based design methods, which are based on variations of 1st- or 2nd-order elastic analyses and ensure strength and reliability on the level of individual components of a structural system. However, with the recent advances and increasing accessibility of structural modeling and analysis tools, combined with the development of affordable desktop computers with the processing and memory capacity required to complete advanced analyses at an acceptable runtime, there has been a growing interest in developing and adopting system-based design methods, which are based on variations of 2nd-order inelastic analyses and ensure strength and reliability on the level of the entire structural system. The main benefit of the system-based design methods is that they explicitly account for most, if not all, component-level limit states directly in the analysis, simplifying or eliminating separate component-level limit state checks while ensuring the overall stability of a structure and accounting for beneficial inelastic load redistribution effects. As the structural engineering profession moves toward broader adoption of system-based design methods, validation, verification, and calibration studies are essential to quantify desired system-level reliabilities and inform the refinement of system-level provisions within future design codes for structural steel buildings. In this study, we investigate system-level reliabilities achieved by two component-based design methods, the Direct Analysis Method and the Advanced Elastic Analysis Method, and two system-based design methods, the Advanced Inelastic Analysis Method and the Direct Design Method. To investigate the system-level reliabilities achieved by these design methods, a series of benchmark structural steel frames were first designed using a structural design optimization framework. System reliability analyses that included uncertainties in geometric properties, material properties, and applied loads were then

performed on the resulting optimal designs using the Importance Sampling technique. The findings of this study indicate that component-based design methods consistently produce system-level reliabilities that exceed target levels of reliability; however, these design methods result in designs that are significantly heavier than those produced by system-based design methods. In contrast, the system-based design methods result in significantly lighter designs, with more consistent levels of reliability that are closer to expected target levels. Based on these findings, recommendations are provided to enhance system-level reliability calibration procedures and to support the effective implementation of system-based design methods in future design codes.

1 INTRODUCTION

For structural engineers, achieving designs that are materially efficient, as well as reliable, is paramount. The ability to achieve such designs depends on the design methods that are available to engineers and their ability to account for geometric and material nonlinearities, while ensuring adequate reliability. In terms of reliability – the focus of this study – we distinguish two categories of design methods: (1) *component-based design methods*, which ensure reliability at the level of individual components of a structural system and deem system failure to occur when the first component fails, and (2) *system-based design methods*, which ensure reliability at the level of the entire structural system and deem system failure to occur when the system's strength is insufficient to resist the applied loads. Although failure can be defined in many other ways related to serviceability, such as the event in which the peak roof or interstorey drift is reached or the maximum rotation capacity is attained, in this study we consider only strength-related limit states. In this study, we investigate two component-based design methods that are implemented in the American Institute of Steel Construction (AISC) 360-22 Specification for Structural Steel Buildings (AISC 2022), the Direct Analysis Method and the Advanced Elastic Analysis Method, and two system-based design methods, the Advanced Inelastic Analysis Method implemented in the AISC 360-22 Specification, and the Direct Design Method being implemented in the next cycle of the Australian and New Zealand design specifications. Detailed descriptions and motivation for the development and implementation of each design method are given in the following sections.

1.1 HISTORICAL DEVELOPMENT AND MOTIVATION

The historical foundation for standardized design in the construction industry in the United States dates back to at least 1923, when the Allowable Stress Design (ASD) framework was introduced in the 1st edition of the AISC Specification (AISC 1923). Until 2005, the ASD framework was based on the principle that stresses developed in a structural member due to nominal service loads must not exceed a certain fraction of the elastic limit, as determined

by a safety factor. The ASD framework attempted to ensure reliability by assigning a sufficiently high factor of safety against failure, thereby addressing uncertainties in geometric properties, material properties, and applied loads implicitly. Although structural steels, including those used in late 19th-century construction, exhibited substantial ductility, early design practice did not include analytical tools or design philosophies capable of explicitly utilizing inelastic strength reserves. As the understanding of structural behavior advanced, plastic design methods emerged, providing upper-bound strength predictions that were significantly higher than elastic estimates and enabling engineers to rationally exploit inelastic strength reserves. However, structural members continued to be designed within the same ASD framework, which could not accommodate these types of material behavior and, as a result, often led to overly conservative and materially inefficient designs.

The lack of a formal approach to account for inelastic material behavior and explicitly ensure reliability within the ASD framework provided the incentive for the development of the Load and Resistance Factor Design (LRFD) framework in the late 1970s and early 1980s (Ellingwood et al. 1980; Galambos 1981). In contrast to the ASD framework, the LRFD framework is based on the ultimate strength of materials, which allows for utilization of both the elastic and plastic stages, and generally leads to more materially efficient designs. More importantly, unlike the ASD framework, in which safety factors were based on engineering judgment to account for uncertainties, the LRFD framework explicitly incorporates uncertainties in geometric properties, material properties, and applied loads, allowing resistance and load factors to be determined statistically by ensuring that target levels of reliability are consistently achieved.

In effect, the introduction of the LRFD framework within any design method – which dictates how structural analysis must be carried out – enables assurance that target levels of reliability are consistently achieved. In component-based design methods, which are typically based on variations of 1st- or 2nd-order elastic (geometrically nonlinear and materially linear) structural analyses and largely govern the current design practice for structural steel buildings, the LRFD framework is applied to individual structural members and connections to ensure reliability at the level of individual components within a structural system. However, with recent advances and the increasing accessibility of structural modeling and analysis tools, combined with the development of affordable desktop computers with the processing and memory capacity required to complete advanced analyses at an acceptable runtime, there has been growing interest in developing and adopting system-based design methods. In these design methods, which are based on variations of 2nd-order inelastic structural analyses, the LRFD framework is applied to the entire structure to ensure

reliability at the system level. This is made possible because the use of 2nd-order inelastic (geometrically and materially nonlinear) structural analyses explicitly accounts for most, if not all, component-level limit states directly in the analysis, simplifying or eliminating separate component-level limit state checks while ensuring overall strength and stability of the structure and accounting for beneficial inelastic load redistribution effects.

Despite the promising advantages of system-based design methods in achieving materially efficient designs of steel structures (Ziemian et al. 1992a; b), their widespread adoption has been hindered by limited guidance on calibration of system-level resistance factors and insufficient data on the actual system-level reliabilities achieved in practice. Several studies have attempted to address this gap: Buonopane and Schafer (2006) evaluated the system-level reliabilities of structural steel frames designed using 2nd-order inelastic analysis and proposed resistance factors based on plastic collapse criteria, Shayan (2013) developed a system reliability analysis framework for determining system-level resistance factors for low- to mid-rise moment-resisting structural steel frames, demonstrating that system-based design methods can provide uniform system-level reliabilities across various system-level failure modes, Zhang et al. (2016a; b) introduced the Direct Design Method and conducted calibration studies for planar gravity-loaded structural steel frames based on simplified system reliability analysis procedures. More recently, studies have extended system-based reliability calibrations to stainless steel frames and spatial structures under combined loading conditions (Arrayago et al. 2022; Arrayago and Rasmussen 2022). Despite these advances, concerns remain as to whether system-based design methods can consistently meet target levels of reliability across a broad range of structural configurations and loading scenarios in practice. For this reason, this study develops a comprehensive framework for evaluating system-level reliability of a wide range of structural steel frames designed using both component- and system-based methods. By comparing the Direct Analysis Method, Advanced Elastic Analysis Method, Advanced Inelastic Analysis Method, and Direct Design Method across a range of benchmark structural steel frames, this research aims to quantify the system-level reliability indices achieved by these design methods, highlight design methods requiring recalibration, and provide recommendations toward broader adoption of system-based design methods in future design codes for structural steel buildings.

1.1.1 Design Criterion for Component-Based Design Methods

If we denote a structural analysis that incorporates all of the requirements of a specific component-based design method and converts applied loads to actions on the structural members by $f(\cdot)$, then the design criterion for a structural member in a structural system designed using the LRFD framework is given by the following inequality:

$$\phi_c R_{nc} \geq f\left(\sum_i \gamma_i q_{n,i}\right), \quad (1)$$

where ϕ_c is the component-level resistance factor corresponding to a limit state governing the response of the structural member, R_{nc} is the nominal strength of the structural member against this limit state, $R_{rc} = f\left(\sum_i \gamma_i q_{n,i}\right)$ is the required strength of the structural member determined from the structural analysis, γ_i represent load factors from the design load combinations that are considered during the design of the structure, and $q_{n,i}$ represent nominal loads acting on the structure. Given that the strength checks, given by Eq. (1), are performed on the level of individual structural components, with component-level resistance factor ϕ_c calibrated to ensure that a target level of component reliability is always achieved, the specific design method is said to be categorized as a component-based design method.

1.1.2 DIRECT ANALYSIS METHOD

In the 6th edition of the AISC Manual of Steel Construction (AISC 1967), two significant improvements were introduced to the AISC's long-standing approach based on the ASD framework: the concept of effective length and implicit consideration of the 2nd-order effects. The concept of effective length was introduced to account for the influence of the stiffness of a structural system on the strength of individual structural members subjected to compression. More specifically, the allowable axial stress was determined using a column strength equation in which an effective length KL replaced the actual unbraced length L. The effective length was obtained from an elastic buckling analysis or, under a prescribed set of assumptions, could be evaluated using alignment charts. For structural members subjected to combined compressive and flexural loads, bending stresses were computed using a 1st-order elastic analysis and subsequently amplified to account for 2nd-order effects through a moment amplification factor incorporated directly into the interaction equations. The compressive stresses appearing in this amplification factor were likewise evaluated using the effective length, thereby maintaining consistency between the treatment of destabilizing effects of compressive and flexural loads.

In the 1st edition of the AISC LRFD Specification for Structural Steel Buildings (AISC 1986), the design approach shifted from the implicit treatment of the 2nd-order effects – previously addressed through a moment amplification factor embedded within the interaction equations – to an explicit and systematic consideration of structural stability. A dedicated chapter on stability was introduced, which clearly stated that *"second-order (P-Δ) effects shall be considered in the design of frames."* Despite this shift, the structural members subjected to compressive loads continued to be designed using the concept of effective length. For structural members subjected to combined

compressive and flexural loads, the required flexural strength in the interaction equations was now to be determined from a 2nd-order elastic analysis. As an alternative to a 2nd-order elastic analysis, a moment amplification procedure – conceptually similar but more robust than that used in the 6th edition of the AISC Manual of Steel Construction – was still permitted. In this procedure, the compressive stresses governing the moment amplification factor continued to be computed using effective lengths, thereby retaining the concept of effective length within the design practice.

A significant shortcoming of the heavy reliance on the concept of effective length within the stability provisions is the difficulty of accurately determining effective lengths for structural members within structural system with complex geometries. For this reason, in the early 2000s, the AISC formed a joint task committee together with the Structural Stability Research Council to develop improved provisions for the design of steel structures that could better account for geometric and material nonlinearities, while simplifying the design process by eliminating the need for the use of effective length. Through a series of studies (Maleck 2001; Deierlein et al. 2002; Martinez-Garcia 2002; Maleck and White 2003; Surovek-Maleck and White 2004a; b; Martinez-Garcia and Ziemian 2006), the joint task committee developed the Direct Analysis Method (DAM), which was formally introduced in the 2005 edition of the AISC 360 Specification (AISC 2005) and remains largely unchanged in its 2022 edition (AISC 2022).

The key advantage of the DAM is that it eliminates the need to compute effective lengths KL. Instead, the DAM uses the unbraced length L of a structural member when determining its nominal compressive strengths P_{nc}. However, in exchange for this simplification, the DAM, which is based on 2nd-order elastic analysis (or geometrically nonlinear analysis with initial system imperfections (GNIA) in European notation), requires (1) to apply a stiffness reduction to the structural members and connections that provide lateral stability to the structural system to account for the effect of yielding, which is often accentuated by the presence of residual stresses, and (2) to account for the initial system imperfections directly in the analysis. The stiffness reduction has two components: (1) a general reduction factor of 0.80 is applied to all cross-sectional stiffnesses, and (2) for heavily compressed members, an additional stiffness reduction factor τ_b is applied to the flexural stiffness EI. Taken together within the design process, the DAM requires a reduction factor of 0.80 to the axial cross-sectional stiffnesses, such that $EA_g \rightarrow 0.80EA_g$, and a reduction factor of $0.80\tau_b$ to the flexural cross-sectional stiffnesses, such that $EI \rightarrow 0.80\tau_b EI$. The initial system imperfections must be included in the analysis either through explicit modeling or, alternatively, using equivalent notional loads.

With reference to Eq. (1), if we denote a structural analysis that incorporates all the requirements of the DAM by $f_{\mathrm{DAM}}(\cdot)$, then the design criterion for a structural member in a structure is given by the following inequality:

$$\phi_c R_{nc} \geq f_{\text{DAM}}\left(\sum_i \gamma_i q_{n,i}\right). \quad (2)$$

Given that the DAM's strength checks in Eq. (2) are performed on the level of each individual structural component of a structural system, the DAM is categorized as a component-based design method.

1.1.3 Advanced Elastic Analysis Method

The DAM relies on defining the unbraced lengths L of structural members subjected to compression, which in some cases might be difficult, if not impossible, to do. As noted in Wang and Ziemian (2019, 2021), examples of structures where this problem arises include, but are not limited to, arches, tree columns, and Vierendeel trusses. Following a series of studies (Nwe Nwe 2014; Giensen Loo 2016; Wang and Ziemian 2019, 2021), a new design method that extends the DAM was developed and introduced in the 2016 edition of the AISC 360 Specification (AISC 2016), termed here the Advanced Elastic Analysis Method (AEAM). This design method addresses conditions in which challenges exist in establishing the unbraced lengths L of structural members. Although the AEAM is similar to the DAM in almost all aspects, the key difference and advantage of the AEAM is that the nominal compressive strength P_{nc} of a structural member can be determined directly from its cross-sectional compressive strength, such that $P_{nc} = F_y A_g$, effectively allowing the unbraced lengths L to be taken as zero. To apply this design method, in addition to the initial system imperfections, an engineer is required to include initial member imperfections by direct modeling in a 2nd-order elastic analysis (or geometrically nonlinear analysis with initial member and system imperfections (GNIA) in European notation). By directly modeling initial member imperfections, the structural analysis captures 2nd-order P-δ effects explicitly, so that the internal moments and stability behavior of the member are represented directly in the analysis, and member capacity can be evaluated using beam-column interaction equations rather than column strength equations based on effective length. Because of this requirement to explicitly model member imperfections, this approach is sometimes also referred to as Direct Modeling of Member Imperfections or DMMI.

With reference to Eq. (1), if we denote a structural analysis that incorporates all the requirements of the AEAM by $f_{\text{AEAM}}(\cdot)$, then the design criterion for a structural member in a structure is given by the inequality of the same form as the one for the DAM shown in Eq. (2):

$$\phi_c R_{nc} \geq f_{\text{AEAM}}\left(\sum_i \gamma_i q_{n,i}\right). \quad (3)$$

The only difference between the design criteria given by Eq. (2) and (3) is that the AEAM, unlike the DAM, requires the initial member imperfections to be directly modeled in the analysis. Otherwise, the AEAM falls within the same category of component-based design methods as the DAM, given that the AEAM's strength checks per Eq. (3), are also performed on the level of individual components.

1.1.4 ADVANCED INELASTIC ANALYSIS METHOD

Due to advances in and the increasing accessibility of nonlinear structural modeling and analysis tools over the past several decades, combined with the development of affordable desktop computers with the processing and memory capacity required to complete advanced analyses at an acceptable runtime, there has been a growing interest in developing and adopting design methods that are based on variations of 2nd-order inelastic analysis. Such design methods can explicitly account for (1) both geometric and material nonlinearities, (2) initial geometric (at both member and system levels) and material (residual stresses) imperfections, and (3) complex but beneficial inelastic load redistribution interactions that occurs between structural members as a structural system approaches its strength limit state. Additionally, design methods based on the 2nd-order inelastic analysis can account for most, if not all, limit states of individual structural members of a structure, thereby simplifying or eliminating separate component-level strength checks while ensuring overall stability of a structural system. As a result, the 2010 edition of the AISC 360 Specification (AISC 2010) introduced a new design method, termed here the Advanced Inelastic Analysis Method (AIAM), which allowed an engineer to design steel structures using 2nd-order inelastic analysis and directly account for the geometric and material imperfections (or geometrically and materially nonlinear analysis with initial geometric (member and system) and material (residual stresses) imperfections (GMNIA) in European notation). It is also worth noting that this design method was not limited to fully restrained (rigid) moment connections, thereby superseding earlier design methods based on the plastic hinge analysis (Beedle 1970).

If we denote the structural analysis that incorporates all the requirements of the AIAM by $f_{\text{AIAM}}(\cdot)$, then the design criterion for an entire structure is given by the following inequality:

$$R_{ns}^{*} \geq f_{\text{AIAM}}\left(\sum\nolimits_{i} \gamma_i q_{n,i}\right), \tag{4}$$

where R_{ns}^{*} is the reduced ultimate strength of the structure and $R_{rs} = f_{\text{AIAM}}\left(\sum_i \gamma_i q_{n,i}\right)$ is the required strength of the structure determined from the analysis. In conducting the 2nd-order inelastic analyses, in which the applied loads are increased incrementally by using a load proportionality factor λ, the reduced ultimate strength of the entire structure can alternatively be denoted using $\lambda_{un}^{*} = R_{ns}^{*}/R_{rs}$ and the design criterion in Eq. (4) can be rewritten into a more convenient form:

$$\lambda_{un}^{*} \geq 1. \tag{5}$$

As can be observed from Eq. (5), no reductions are applied directly to the ultimate strength λ_{un}^{*}. Instead, in attempt to account for uncertainties and achieve an acceptable level of system reliability when using the AIAM, the AISC 360-22 Specification requires a reduction factor of 0.90 to be applied to the material properties – elastic modulus E and

yield stress F_y – of structural members when performing the analysis. Thus, the ultimate strength λ_{un}^{*} obtained during the design process according to the AIAM is not the actual strength of a structure but is reduced due to the reduction factor of 0.90 already embedded in the structural analysis. However, as noted in the Commentary to Appendix 1 of the AISC 360-22 Specification, this reduction factor is assumed to be conservative, and no system reliability analyses were performed to calibrate it. The AIAM can be categorized as a system-based design method because it performs a strength check, given by Eq. (5), on the level of the entire structural system. However, it remains uncalibrated and, thus, does not guarantee that any particular level of target reliability is always achieved, further highlighting the need for the present study.

1.1.5 DIRECT DESIGN METHOD

To address the limitations of the AIAM – namely, its inability to ensure that a target level of system reliability is always achieved – Zhang et al. (2016a; b) proposed a new design method based on 2nd-order inelastic analysis (or geometrically and materially nonlinear analysis with initial geometric (member and system) and material (residual stresses) imperfections (GMNIA) in European notation), termed the Direct Design Method (DDM), which, unlike the AIAM, does not require an engineer to apply any reductions during the analysis process, thus simplifying the design process by allowing an engineer to model a structure "as is." To ensure that an acceptable level of system reliability is achieved, the DDM employs a system-level resistance factor ϕ_s that is applied to the nominal ultimate strength of a structure, such that the design criterion is given by

$$\phi_s R_{ns} \geq f_{\mathrm{DDM}}\left(\sum_i \gamma_i q_{n,i}\right), \tag{6}$$

which, alternatively, can be rewritten as

$$\phi_s \lambda_{un} \geq 1. \tag{7}$$

In the DDM, any target level of reliability can be, in principle, achieved by calibrating ϕ_s in Eq. (7) through rigorous system reliability analysis. Such analysis was performed by Zhang et al. (2016a; b) who recommended using ϕ_s of 0.85 for low- and mid-rise structural steel frames, a value which is used in this study, based on nominal loads and load factors obtained from the ASCE 7-22 Standard (ASCE 2021). This calibration corresponds to a system-level reliability index β of 2.9 for structural steel frames subjected to gravity loads only and 2.7 for structural steel frames subjected to combined gravity and wind loads. When using the nominal loads and load factors specified in the AS/NZS 1170 Standard (Standards Australia 2002a; b) ϕ_s of 0.90 is obtained for the gravity loads only combination, corresponding to system-level reliability indices β of 3.0 and 3.2 for planar and spatial steel frames, respectively. The ϕ_s of 0.90 is used in the draft revised Australian standard for steel structures (AS4100, 2026) and is the same system resistance

factor as that previously implemented in the Australian and New Zealand design standards for cold-formed steel structures AS/NZS 4600 (Standards Australia 2018), steel storage racks AS/NZS 4084.1 (Standards Australia 2023a) and formwork structures AS/NZS 3610.2 (Standards Australia 2023b). For this reason, in addition to studying the system-level reliabilities achieved by the DDM with $\phi_s = 0.85$ ($\lambda_{un} \geq 1.18$), the system-level reliabilities achieved by the DDM with $\phi_s = 0.90$ ($\lambda_{un} \geq 1.11$) are also studied herein. To distinguish between these two implementations, the DDM with $\phi_s = 0.85$ and $\phi_s = 0.90$ are referred to as DDM85 and DDM90, respectively.

1.2 General Procedure

To investigate the system-level reliabilities achieved by the considered design methods, a series of benchmark structural steel frames were first designed using a structural design optimization framework and analyzed using 2nd-order inelastic analysis. System reliability analyses that included uncertainties in geometric properties, material properties, and applied loads were then performed on the ultimate strengths of the resulting optimal designs using the Importance Sampling technique. This general procedure enabled consistent comparison between the system-level reliabilities achieved by the design methods of interest.

2 Design Process

2.1 Structural Steel Frames of Interest

To investigate the system reliabilities achieved by the considered design methods, the structural steel frames presented in Ziemian and Ziemian (2021) are selected for comparison. These structural steel frames, presented in Fig. 1, represent a wide range of geometric configurations, showcasing varying sensitivities to geometric and material nonlinearities. In all frames, the structural members are oriented to experience flexure about their major axes, except for structural steel frames #8 and #10 in which the columns are oriented to experience flexure about their minor axes. The structural steel frames are also assumed to be fully braced out-of-plane, allowing for fully planar analyses and precluding spatial effects. This approach is justified by system reliability studies which demonstrated that planar and spatial frames have nearly identical system-level reliability indices when designed by the DDM (Liu 2016; Liu et al. 2019). While the load magnitudes provided by Ziemian and Ziemian (2021) are retained for further design according to the design methods considered in this study, the elastic moduli E and yield stresses F_y for all frames are assumed to be 200 GPa (29,000 ksi) and 345 MPa (50 ksi), respectively. The magnitudes of the loads applied to the benchmark structural steel frames can be found in the Supplementary Materials.

2.2 DESIGN LOADS AND LOAD COMBINATIONS

Instead of considering only one load combination per structural steel frame during the design process, as was done in Ziemian and Ziemian (2021), we consider the following set of load combinations from the American Society of Civil Engineers (ASCE) Standard for Minimum Design Loads and Associated Criteria for Buildings and Other Structures (ASCE 2021), with their references in the Standard provided, given that the benchmark structural steel frames, collectively, are subjected to various combinations of dead D_n, floor live L_{fn}, roof live L_{rn}, and wind W_n loads:

$$\begin{cases} \text{1a:} & 1.4D_n \\ \text{2a:} & 1.2D_n + 1.6L_{fn} + 0.5L_{rn} \\ \text{3a.1:} & 1.2D_n + 0.5L_{fn} + 1.6L_{rn} \\ \text{3a.2:} & 1.2D_n + 1.6L_{rn} + 0.5W_n \\ \text{4a:} & 1.2D_n + 0.5L_{fn} + 0.5L_{rn} + 1.0W_n \\ \text{5a:} & 0.9D_n + 1.0W_n \end{cases}, \tag{8}$$

For the work reported here, we assume that roof live loads L_{rn} and floor live loads L_{fn} are statistically identical, and no distinction is made between the two. Accordingly, the load factors for floor live loads γ_{L_f} are used in place of those for roof live loads γ_{L_r}. This assumption has been adopted in several previous studies investigating system reliabilities achieved by various design methods (Zhang et al. 2016a; b, 2018; Liu et al. 2019; Akchurin et al. 2025) and provides an important frame of reference for comparative evaluation. Recent studies that have focused on providing statistically supported load models for roof live loads L_{fn} (Karasu et al. 2022, 2025) suggest that this assumption may be overly conservative. However, the explicit incorporation of these recent roof load models is beyond the scope of the present study and is therefore not pursued here. The authors intend to revisit this assumption in future work as improved data become available. Under this assumption, the set of considered load combinations in Eq. (8) can be rewritten as

$$\begin{cases} \text{1a:} & 1.4D_n \\ \text{2a:} & 1.2D_n + 1.6L_{fn} + 1.6L_{rn} \\ \text{3a.1:} & 1.2D_n + 0.5L_{fn} + 0.5L_{rn} \\ \text{3a.2:} & 1.2D_n + 0.5W_n \\ \text{4a:} & 1.2D_n + 0.5L_{fn} + 0.5L_{rn} + 1.0W_n \\ \text{5a:} & 0.9D_n + 1.0W_n \end{cases}, \tag{9}$$

Observing that load combination 4a always controls over load combinations 3a.1, 3a.2, and 5a, the set of considered load combinations in Eq. (9) finally simplifies to

$$\begin{cases} \text{1a:} & 1.4D_n \\ \text{2a:} & 1.2D_n + 1.6L_{fn} + 1.6L_{rn} \\ \text{4a:} & 1.2D_n + 0.5L_{fn} + 0.5L_{rn} + 1.0W_n \end{cases}, \tag{10}$$

which is used during the design of all 22 structural steel frames according to all considered design methods.

Current design codes do not explicitly stipulate whether proportional or nonproportional loading should be used during the design process when lateral loads are present. Therefore, this study considers both approaches to provide engineers

with additional insight into how the choice of load proportionality affects the design process and the resulting system-level reliabilities.

2.3 SECTION SELECTION

The structural analyses used to design the structural steel frames were performed using line finite elements, which are incapable of capturing member limit states associated with cross-sectional instabilities, such as local buckling. For this reason, the selection of sections was restricted to W-shaped sections listed in the 16th edition of the AISC Steel Construction Manual (AISC 2023) that are classified as both compact in flexure about both major and minor axes and nonslender in axial compression, as specified by the requirements of Chapter B of the AISC 360-22 Specification. This restriction ensures that the sections used in the final designs of the structural steel frames can reach their plastic capacity and generally develop a normalized rotation capacity of 3 before cross-sectional instabilities occur, thereby justifying the use of line finite elements in the conducted structural analyses. Out of the 289 W-shaped sections listed in the AISC Steel Construction Manual, 168 were found to be compact in flexure about both the major and minor axes and nonslender in axial compression. Additionally, following standard practice, the selection of sections for columns was further restricted to W8X… through W14X… sections. As a result, during the design of the structural steel frames according to the considered design method, 168 sections were available for the selection of beams and braces, and 72 sections were available for the selection of columns.

2.4 DESIGN CRITERIA AND LIMIT STATES

In this study, the scope of the design is restricted to limit states of structural members only and connection limit states are not considered. Instead, beam-to-column connections are idealized as either perfectly pinned or fully rigid, consistent with common practice in prior system reliability studies of structural steel frames. This modeling choice is intended to isolate and examine the baseline structural response of the structural steel frames without the added complexity associated with connection behavior. Recent work has begun to explore the role of partially restrained connections within the context of the DDM (Liu 2019; Zhu et al. 2019; Yan and Rasmussen 2021). Incorporating such effects into system reliability-based design remains an important topic for future research but is beyond the scope of the present study.

For component-based design methods – DAM and AEAM – we consider three possible limit states for each structural member:

1. If a structural member is subjected to pure tensile load, such that $P_r > 0$ and $M_r = 0$, the design criteria in Eq. (2) and (3) can be rewritten as

$$\phi_{ct} P_{nt} \geq |P_r|, \tag{11}$$

where ϕ_{ct} is the component-level resistance factor related to the tensile yielding in the gross cross-section of the structural member and is equal to 0.90, and P_{nt} is the nominal tensile strength of the structural member determined in accordance with Chapter D of the AISC 360-22 Specification.

2. If a structural member is subjected to pure compressive load, such that $P_r < 0$ and $M_r = 0$, the design criteria in Eq. (2) and (3) can be rewritten as

$$\phi_{cc} P_{nc} \geq |P_r|, \tag{12}$$

where ϕ_{cc} is the component-level resistance factor related to the compressive buckling of the structural member and is equal to 0.90, and P_{nc} is the nominal compressive strength of the structural member determined in accordance with Chapter E of the Specification. For the DAM, P_{nc} is computed with $K = 1$ and, for the AEAM, P_{nc} is computed as $F_y A_g$.

3. If a structural member is subjected to combined axial and flexural load, such that $|P_r| \geq 0$ and $M_r \neq 0$, the design criteria in Eq. (2) and (3) can be rewritten as

$$\begin{cases} \dfrac{|P_r|}{P_c} + \dfrac{8}{9}\dfrac{|M_r|}{M_c} \leq 1, & \dfrac{|P_r|}{P_c} \geq 0.2 \\ \dfrac{1}{2}\dfrac{|P_r|}{P_c} + \dfrac{|M_r|}{M_c} \leq 1, & \dfrac{|P_r|}{P_c} < 0.2 \end{cases}, \tag{13}$$

where P_c is the available axial design strength, either tensile or compressive depending on whether the structural member is experiencing pure tension or compression, and $M_c = \phi_{cb} M_n$ is the available flexural design strength with ϕ_{cb} being the component-level resistance factor related to the yielding due to flexure and is equal to 0.90, and M_n is the nominal flexural strength determined in accordance with Chapter F of the AISC 360-22 Specification. In all cases, members are assumed as fully braced out-of-plane resulting in the nominal flexural strength taken as $M_n = M_p$.

Combined, the limit states given by Eq. (11), (12), and (13) constitute the design criteria, denoted by s_i^j, which must be satisfied for each structural member i for each load combination j considered during the design process, given by

$$s_i^j = \begin{cases} \left|P_{r,i}^j\right| - \phi_{ct} P_{nt,i} \leq 0, & P_{r,i}^j > 0 \text{ and } M_{r,i}^j = 0 \\ \left|P_{r,i}^j\right| - \phi_{cc} P_{nc,i} \leq 0, & P_{r,i}^j < 0 \text{ and } M_{r,i}^j = 0 \\ \dfrac{\left|P_{r,i}^j\right|}{P_{c,i}} + \dfrac{8}{9}\dfrac{\left|M_{r,i}^j\right|}{M_{c,i}} - 1 \leq 0, & \dfrac{\left|P_{r,i}^j\right|}{P_{c,i}} \geq 0.2 \text{ and } \left|M_{r,i}^j\right| \neq 0 \\ \dfrac{1}{2}\dfrac{\left|P_{r,i}^j\right|}{P_{c,i}} + \dfrac{\left|M_{r,i}^j\right|}{M_{c,i}} - 1 \leq 0, & \dfrac{\left|P_{r,i}^j\right|}{P_{c,i}} < 0.2 \text{ and } \left|M_{r,i}^j\right| \neq 0 \end{cases}, \tag{14}$$

where the required strength P_r and M_r are determined from the 2nd-order elastic analysis.

Similarly, for the system-based design methods – AIAM and DDM – the design criteria, denoted by s^j, are simply given by Eq. (5) for the AIAM and Eq. (7) for the DDM. These design criteria are checked for each load combination j considered during the design process. For the AIAM, the design criterion is given by

$$s^j = 1 - \lambda_{un}^{*j} \leq 0, \tag{15}$$

and, for the DDM, the design criterion is given by

$$s^j = 1 - \phi_s \lambda_{un}^{j} \leq 0, \tag{16}$$

where the ultimate strengths λ_{un}^{*} (AIAM) and λ_{un} (DDM) are determined from the 2nd-order inelastic analysis.

2.5 STRUCTURAL DESIGN OPTIMIZATION

For a robust investigation of the system-level reliabilities achieved by the considered design methods, it is important to obtain the most optimal designs of the benchmarks structural steel frames, with least possible weight, that satisfy all the requirements of each considered design methods. In doing so, we attempt to ensure that a minimum level of system reliability will be explored for each design method and structural steel frame of interest. While it is possible to achieve such optimal designs manually through a trial-and-error approach for simple structural steel frames with only a few structural members, this approach quickly becomes impractical for more complex structural steel frames with many structural members. To address this challenge, we have developed and employed a structural design optimization framework to systematically identify the designs with least possible weight that meet all the requirements of each considered design method, which serve as constraints in the structural design optimization problem at hand.

In general, the process of structural design can be formulated as a well-posed mathematical optimization problem, where the weight $W = W(\vec{p})$ of a structure must be minimized with respect to the parameters $\vec{p}$ that describe the structure and serve as the design variables. In the case of this study, the parameters $\vec{p}$ are the cross-sectional dimensions and properties of the W-shaped sections available for selection during the design of the benchmark structural steel frames and, thus, the structural design optimization problem at hand is discrete in nature. For this reason, it is convenient to introduce a new set of N_{SM} integer design variables $\vec{\alpha}$, where N_{SM} is the number of structural members in a structural steel frame of interest, with respect to which the optimization will be performed, such that $\vec{p} = \vec{p}(\vec{\alpha})$ and $W = W(\vec{\alpha})$. In effect, the i^{th} component of the design vector $\vec{\alpha}$ defines the W-shaped section that will be prescribed to the i^{th} structural member of a structural steel frame from the list of sections available for selection.

2.5.1 CONSTRAINTS

2.5.1.1 STRENGTH CONSTRAINTS

As mentioned earlier, the structural design optimization should not only result in optimal designs, with least possible weight, but also satisfy the requirements – *strength constraints* – imposed by each design method and given by the design criteria in Eq. (14), (15), and (16).

2.5.1.2 CONSTRUCTABILITY CONSTRAINTS

In this study, serviceability limit states are not imposed as an additional set of constraints in the structural design optimization framework, as they typically dominate the design process by imposing, albeit implicitly, much stricter constraints on the overall stiffness of a structure than the strength constraints. However, we do incorporate *constructability constraints* to ensure geometric compatibility between the structural members at the connection locations, which are typically omitted in the previous studies on the structural design optimization. In this study, the three types of constructability constraints shown in Fig. 2 are considered:

1. At the beam-to-column connections, if the column is oriented to bend about its major axis, the flange width of the column $b_{f,c}$ must be greater than or equal to the flange width of the beam $b_{f,b}$.
2. At the beam-to-column connections, if the column is oriented to bend about its minor axis, the web depth of the column $d_c - 2t_{f,c}$ must be greater than or equal to the flange width of the beam $b_{f,b}$.
3. At the column-to-column connections, both the depth d_{bc} and flange width $b_{f,bc}$ of the bottom column must be greater than or equal to the depth d_{tc} and flange width $b_{f,tc}$ of the top column.

If there are N_{BCC} beam-to-column connections in a structure, the constructability constraints at the k^{th} beam-to-column connection, denoted by $c_1^k = c_1^k(\vec{\alpha})$, can be expressed as

$$c_1^k = \begin{cases} b_{f,b} - b_{f,c} \le 0, & \text{column bending about major axis} \\ b_{f,b} - \left(d_c - 2t_{f,c}\right) \le 0, & \text{column bending about minor axis'} \end{cases} \tag{17}$$

and, similarly, if there are N_{CCC} column-to-column connections in a structure, the constructability constraints at the ℓ^{th} column-to-column connection, denoted by $c_2^\ell = c_2^\ell(\vec{\alpha})$ and $c_3^\ell = c_3^\ell(\vec{\alpha})$, can be expressed as

$$c_2^\ell = d_{tc} - d_{bc} \le 0, \tag{18}$$

$$c_3^\ell = b_{f,tc} - b_{f,bc} \le 0. \tag{19}$$

2.5.1.3 SYMMETRY CONSTRAINTS

In addition to constructability constraints, following standard practice, we also impose *symmetry constraints*. These constraints allow us to assign the same section to different groups of structural members, thereby reducing the number of unique sections required for construction of a particular structural steel frame. For example, it is common to assign identical sections to the inner and outer beams of each floor, as well as to the inner and outer columns. While symmetry

can, in principle, be enforced through explicit equality constraints of the form $\alpha_i = \alpha_j$ if two structural members i and j share the same section, such constraints are difficult to handle efficiently within the Genetic Algorithm used as the optimizer in the developed structural design optimization framework. To address this issue, we introduce a new set of N_{IDV} independent integer design variables $\vec{\omega}$, where $N_{\mathrm{IDV}} \leq N_{\mathrm{SM}}$ is the number of independent design variables $\vec{\omega}$, with the original design variables $\vec{\alpha}$ becoming dependent on $\vec{\omega}$ via a predefined function $\vec{\alpha} = m(\vec{\omega})$ that maps the independent to dependent design variables. The introduction of the independent design variables $\vec{\omega}$ allows us to mimic the equality constraints and automatically satisfy them by ensuring that two structural members i and j share the same section if they are assigned the same independent design variable ω_k, such that $\alpha_i = \alpha_j = \omega_k$. The introduction of the independent design variables $\vec{\omega}$ provides two additional key benefits: (1) it reduces the dimensionality of the structural design optimization problem by grouping structural members into categories governed by a single independent design variable, and (2) it reduces the number of unique constructability constraints that must be satisfied for a given structural steel frame by reducing the number of unique beam-to-column and column-to-column connections.

The mapping between the independent and dependent design variables for structural steel frames #1 to #11 with irregular geometries can be found in the Supplementary Materials. The inner beams, outer beams, inner columns, and outer columns are assumed to have the same section every two floors for structural steel frames #12 to #19, every three floors for structural steel frames #20 and #21, and every four floors for frame #22.

2.5.2 GENETIC ALGORITHM

To summarize, the structural design optimization problem can be formulated mathematically as:

$$
\begin{aligned}
&\text{minimize} && W = \rho \sum_{i=1}^{N_{\mathrm{SM}}} L_i A_{g,i}(\vec{\omega}) \text{ with respect to } \vec{\omega}, && \\
&\text{subject to} && \textit{Box constraints} && \\
&&& \text{For beams and braces:} \quad 1 \leq \omega_i \leq 168, && \\
&&& \text{For columns:} \quad 1 \leq \omega_i \leq 72, && i \in \{1, \ldots, N_{\mathrm{IDV}}\}, \\
&&& \textit{Strength constraints} && \\
&&& \text{For DAM:} && \\
&&& s_i^j(\vec{\omega}) \leq 0 \text{ in Eq. (14)}, && i \in \{1, \ldots, N_{\mathrm{SM}}\}, \\
&&& \text{For AEAM:} && \\
&&& s_i^j(\vec{\omega}) \leq 0 \text{ in Eq. (14)}, && j \in \{1, \ldots, N_{\mathrm{DLC}}\}, \\
&&& \text{For AIAM:} && \\
&&& s^j(\vec{\omega}) \leq 0 \text{ in Eq. (15)}, && j \in \{1, \ldots, N_{\mathrm{DLC}}\}, \\
&&& \text{For DDM:} && \\
&&& s^j(\vec{\omega}) \leq 0 \text{ in Eq. (16)}, && \\
&&& \textit{Constructability constraints} && \\
&&& \text{For beam-to-column connections:} && \\
&&& c_1^k(\vec{\omega}) \leq 0 \text{ in Eq. (17)}, && k \in \{1, \ldots, N_{\mathrm{BCC}}\}, \\
&&& \text{For column-to-column connections:} && \\
&&& c_2^\ell(\vec{\omega}) \leq 0 \text{ in Eq. (18)}, && \ell \in \{1, \ldots, N_{\mathrm{CCC}}\}, \\
&&& c_3^\ell(\vec{\omega}) \leq 0 \text{ in Eq. (19)}, &&
\end{aligned}
\tag{20}
$$

where ρ is the density of structural steel assumed to be 8000 kg/m^3 (0.290 lb/in.^{3}), L_i is the length of the i^{th} structural member, and N_{DLC} is the number of design load combinations considered during the design process and is equal to 3 in the present study.

The structural design optimization problem formulated in Eq. (20) was solved using the Genetic Algorithm (GA) (Goldberg 2012) implemented in the `Metaheuristics.jl` package (Mejía-de-Dios and Mezura-Montes 2022), an open-source package written in the Julia programming language that implements several global optimization metaheuristic algorithms for solving single- and multi-objective optimization problems. A key distinction of the implementation of the GA in the `Metaheuristics.jl` package, compared to other implementations that typically rely on the Penalty Method to guide the algorithm toward the constrained optimum, is its use of the Constrained Violation Rule (Deb 2000). Unlike the Penalty Method, which penalizes the objective function for constraint violations, the Constrained Violation Rule computes the average constraint violation to perform pairwise comparisons of individuals in the population during the selection process; thus, enabling the algorithm to focus on feasibility during the optimization process without relying on arbitrary penalty parameters. Moreover, the Constrained Violation Rule ensures that the entire population will reach the feasible region if at least one feasible solution is identified or provided. In the used structural design optimization framework, the Binary Tournament Selection was used as the selection operator to ensure that fitter individuals had a higher probability of being chosen while maintaining diversity within the population, the Simulated Binary Crossover (Deb and Agrawal 1995) was used as the crossover operator to generate offspring solutions by combining the genetic material of parent solutions in a way that encourages exploration of the design space, and the Polynomial Mutation (Deb and Deb 2014) was used as the mutation operator to introduce small and controlled variations to individual solutions, thus improving the algorithm's ability to escape local optima. Additionally, an elitist strategy was used to ensure that the fittest individuals from the current generation were carried over to the next, thereby preserving high-quality solutions throughout the structural design optimization process. Note that while many other options exist for the selection, crossover, and mutation operators, the described setup had demonstrated the best convergence rates.

2.5.3 Finite Element Modeling and Analysis

For the purposes of the structural design optimization, the 2nd-order elastic and inelastic analyses were performed using `OpenSeesPy`, an open-source Python package for finite element analysis (McKenna et al. 2010). For designs according to the component-based design methods, elastic beam-column finite elements based on Euler-Bernoulli beam theory were used to model the structural members, and for designs according to the system-based design methods, which explicitly consider material nonlinearities, displacement-based finite elements with fiber-type sections. The material assigned to the structural members was modeled using elastic-perfectly plastic constitutive

model. In all cases, each structural member was discretized into four finite elements. For the 2nd-order inelastic analyses for the AIAM and DDM, similar to the approach used in Zhang et al. (2016a; b), the European Convention for Constructional Steelwork's self-equilibrating residual stress pattern was adopted.

Following Ziemian and Ziemian (2021), for structural steel frames with multiple lean-on columns, the lean-on columns were modeled as a single column line on each side of the structural steel frame. The initial nominal frame out-of-plumbness imperfections ψ_n with magnitude 1/500 were modeled directly in the directions indicated in Fig. 1 to avoid the development of fictitious shear forces and moments during the analyses. For the AEAM, AIAM, and DDM, the initial nominal member out-of-straightness imperfections δ_n of magnitude $L/1000$ were also modeled directly: to induce the largest 2nd-order P-δ effects beams were assumed to have downward camber and columns were assumed to have camber in the direction opposite to the applied wind loads (i.e., to the right for leftward wind loads and to the left for rightward wind loads).

For proportional loading designs, gravity and wind loads were increased simultaneously while maintaining a constant load ratio. For nonproportional loading designs, a sequential procedure was adopted: frames subjected to gravity loads only were analyzed using a pushdown analysis in which the gravity loads were increased to failure, whereas frames subjected to combined gravity and wind loads were analyzed using a pushover analysis in which the gravity loads were applied first and the wind loads were then increased to failure.

To appropriately account for potentially large deflections during the exploration of the design space by the GA, the corotational geometric transformation was used in the analyses according to all considered design methods. For the DAM and AEAM, the Load Control Method was employed to incrementally apply the loads, while for the AIAM and DDM, the Arclength Control Method was used.

2.6 PROCEDURE

For each benchmark structural steel frame, the structural design process according to a design method of interest was performed using the following procedure:

1. A set of 1,000 initial candidate designs was created by generating 1,000 random independent design vectors $\vec{\omega}$ to establish the initial population in the GA.
2. For each candidate design in a population, (1) its independent design variables $\vec{\omega}$ were mapped to dependent design variables $\vec{\alpha}$, (2) cross-sectional dimensions and properties $\vec{p}$ were extracted, (3) objective function value W – weight – was computed, (4) strength constraint values $\vec{S}$ were computed by performing either 2nd-

order elastic or inelastic analysis based on the design method of interest, (5) constructability constraint values $\vec{C}$ were computed, (6) average constraint violation values were computed, and (7) passed back to the GA.

3. Based on the values of the objective function and average constraint violation of all candidate designs in the current generation, the GA generated the next generation of candidate designs by applying selection, crossover, and mutation operators on the independent design vectors $\vec{\omega}$.
4. Steps 2 and 3 were repeated until the whole population converged to the final solution – optimal design of the structural steel frame, with least possible weight, that meets all the requirements of the design method of interest.

Note that the described procedure is general and can be applied to any design method, including those not considered in the present study. The only step that is different is the computation of strength constraints, which differs between the design methods. Additional flowcharts describing the step-by-step procedure of computing the strength constraints – the most computationally intensive part of the structural design optimization – for each of the considered design methods can be found in the Supplementary Materials. Results of the final optimal designs for the benchmark structural steel frames designed according to the design methods of interest are provided in Section 4.

3 System Reliability Analysis

3.1 Limit State Function Formulation

For the purposes of system reliability analysis, failure of a structure is defined as the event in which the structure reaches its ultimate strength under a given random load combination. In the structural analyses performed in this study, the ultimate strength of a structure is defined by the ultimate random load proportionality factor $\boldsymbol{\lambda_u}$ that the structure can sustain before total loss of its load-carrying capacity, such that $\boldsymbol{\lambda_u}$ is less than unity. This definition of failure is based on strength considerations only as no serviceability-related limit states, such as interstorey drift or roof displacement limits, are not considered during the design process. Accordingly, the limit state function for a single random load combination is given by

$$g(\vec{\boldsymbol{X}}) = \boldsymbol{\lambda_u}(\vec{\boldsymbol{X}}) - 1, \tag{21}$$

where $\boldsymbol{\lambda_u}$ is obtained from a 2nd-order inelastic analysis with random loads applied using nonproportional loading that better represents the real-life loading conditions, and $\vec{\boldsymbol{X}}$ is the vector of N_{RV} random variables associated with uncertainties in geometric properties, material properties, and applied loads that fully define the system reliability problem for the structure.

If there are N_{RLC} random load combinations that must be considered for the structure, then the failure of the structure is defined as an event in which the ultimate random strength is insufficient to resist the random loads associated with any of the considered random loads, such that the limit state function is given by

$$G(\vec{\boldsymbol{X}}) = \min\{g_1(\vec{\boldsymbol{X}}), \dots, g_{N_{\mathrm{RLC}}}(\vec{\boldsymbol{X}})\}, \tag{22}$$

which effectively represents a typical limit state function for series systems, where system failure occurs when any one of its failure modes is reached. In the case of this study, a failure mode of a system refers to the failure of a structure under one of the considered random load combinations.

3.2 RANDOM LOAD COMBINATIONS

The benchmark structural steel frames, collectively, are subjected to various combinations of dead D_n, floor live L_{fn}, roof live L_{rn}, and wind W_n loads; therefore, the random demand $\boldsymbol{Q}(\vec{x}, t)$ on a frame can be represented as a linear combination of random processes associated with dead $\boldsymbol{D}(\vec{x}, t)$, floor live $\boldsymbol{L_f}(\vec{x}, t)$, roof live $\boldsymbol{L_r}(\vec{x}, t)$, and wind $\boldsymbol{W}(\vec{x}, t)$ loads, such that

$$\boldsymbol{Q}(\vec{x}, t) = \boldsymbol{D}(\vec{x}, t) + \boldsymbol{L_f}(\vec{x}, t) + \boldsymbol{L_r}(\vec{x}, t) + \boldsymbol{W}(\vec{x}, t). \tag{23}$$

Estimating the statistics of these random processes is a challenging task given that they exhibit space and time dependence, except for the dead load $\boldsymbol{D}(\vec{x}, t)$. For this reason, numerous load combination models were developed over the years to address this issue, among which Turkstra's Rule (Turkstra and Madsen 1980) is the simplest and most practical, and as such, serves as the foundation for the LRFD methods' load combinations (Ellingwood et al. 1980; McAllister et al. 2025). Turkstra's Rule assumes that when a load reaches its maximum value in the design lifetime of a structure, other loads are most likely to be at their arbitrary point-in-time values. Applying Turkstra's Rule to Eq. (23) allows us to remove the dependence on space and time by converting the random processes into arbitrary point-in-time $(\cdot)_{apt}$ and lifetime maximum $(\cdot)_{max}$ random variables, resulting in the following set of the random load combinations:

$$\begin{cases} 1: & \boldsymbol{D_{max}} + \boldsymbol{L_{f,apt}} + \boldsymbol{L_{r,apt}} + \boldsymbol{W_{apt}} \\ 2: & \boldsymbol{D_{apt}} + \boldsymbol{L_{f,max}} + \boldsymbol{L_{r,apt}} + \boldsymbol{W_{apt}} \\ 3: & \boldsymbol{D_{apt}} + \boldsymbol{L_{f,apt}} + \boldsymbol{L_{r,max}} + \boldsymbol{W_{apt}} \\ 4: & \boldsymbol{D_{apt}} + \boldsymbol{L_{f,apt}} + \boldsymbol{L_{r,apt}} + \boldsymbol{W_{max}} \end{cases}. \tag{24}$$

Due to the inherently low variability of the dead load, it is assumed that the arbitrary point-in-time dead load $\boldsymbol{D_{apt}}$ and lifetime maximum dead load $\boldsymbol{D_{max}}$ are the same, such that $\boldsymbol{D} = \boldsymbol{D_{apt}} = \boldsymbol{D_{max}}$. For simplicity, it is also assumed that the contribution of the arbitrary point-in-time wind load $\boldsymbol{W_{apt}}$ is negligible given that its expected value is close to zero (Ellingwood et al. 1980). Applying these assumptions and factoring out the nominal load, the set of random load combinations in Eq. (24) simplifies to

$$\begin{cases} 1: & \boldsymbol{X_D} D_n + \boldsymbol{X}_{\boldsymbol{L_f}}^{\boldsymbol{apt}} L_{fn} + \boldsymbol{X}_{\boldsymbol{L_r}}^{\boldsymbol{apt}} L_{rn} \\ 2: & \boldsymbol{X_D} D_n + \boldsymbol{X}_{\boldsymbol{L_f}}^{\boldsymbol{max}} L_{fn} + \boldsymbol{X}_{\boldsymbol{L_r}}^{\boldsymbol{apt}} L_{rn} \\ 3: & \boldsymbol{X_D} D_n + \boldsymbol{X}_{\boldsymbol{L_f}}^{\boldsymbol{apt}} L_{fn} + \boldsymbol{X}_{\boldsymbol{L_r}}^{\boldsymbol{max}} L_{rn} \\ 4: & \boldsymbol{X_D} D_n + \boldsymbol{X}_{\boldsymbol{L_f}}^{\boldsymbol{apt}} L_{fn} + \boldsymbol{X}_{\boldsymbol{L_r}}^{\boldsymbol{apt}} L_{rn} + \boldsymbol{X}_{\boldsymbol{W}}^{\boldsymbol{max}} W_n \end{cases}, \tag{25}$$

where $\boldsymbol{X_D} = \boldsymbol{D}/D_n$, $\boldsymbol{X}_{\boldsymbol{L_f}}^{\boldsymbol{apt}} = \boldsymbol{L}_{\boldsymbol{f,apt}}/L_{fn}$, $\boldsymbol{X}_{\boldsymbol{L_f}}^{\boldsymbol{max}} = \boldsymbol{L}_{\boldsymbol{f,max}}/L_{fn}$, $\boldsymbol{X}_{\boldsymbol{L_r}}^{\boldsymbol{apt}} = \boldsymbol{L}_{\boldsymbol{r,apt}}/L_{rn}$, $\boldsymbol{X}_{\boldsymbol{L_r}}^{\boldsymbol{max}} = \boldsymbol{L}_{\boldsymbol{r,max}}/L_{rn}$, and $\boldsymbol{X}_{\boldsymbol{W}}^{\boldsymbol{max}} = \boldsymbol{W}_{\boldsymbol{max}}/W_n$ are the normalized random variables associated with the dead, arbitrary point-in-time floor live, lifetime maximum floor live, arbitrary point-in-time roof live, lifetime maximum roof live, and lifetime maximum wind loads, respectively.

As discussed earlier in the context of design load combinations and consistent with prior system reliability studies (Zhang et al. 2016a; b, 2018; Liu et al. 2019; Akchurin et al. 2025), we assume that random roof live loads $\boldsymbol{L_r}$ are statistically equivalent to random floor live loads $\boldsymbol{L_f}$, and no distinction is made between the two. This assumption simplifies the formulation of the random load combinations while remaining aligned with existing practice; the implications of this assumption will be examined in future work. At the same time, the described probabilistic framework for formulation of the random load combinations is retained to facilitate future studies. Under this assumption, the set of considered random load combinations in Eq. (25) can be rewritten as

$$\begin{cases} 1: & \boldsymbol{X_D} D_n + \boldsymbol{X}_{\boldsymbol{L_f}}^{\boldsymbol{apt}} L_{fn} + \boldsymbol{X}_{\boldsymbol{L_f}}^{\boldsymbol{apt}} L_{rn} \\ 2: & \boldsymbol{X_D} D_n + \boldsymbol{X}_{\boldsymbol{L_f}}^{\boldsymbol{max}} L_{fn} + \boldsymbol{X}_{\boldsymbol{L_f}}^{\boldsymbol{max}} L_{rn} \\ 3: & \boldsymbol{X_D} D_n + \boldsymbol{X}_{\boldsymbol{L_f}}^{\boldsymbol{apt}} L_{fn} + \boldsymbol{X}_{\boldsymbol{L_f}}^{\boldsymbol{apt}} L_{rn} \\ 4: & \boldsymbol{X_D} D_n + \boldsymbol{X}_{\boldsymbol{L_f}}^{\boldsymbol{apt}} L_{fn} + \boldsymbol{X}_{\boldsymbol{L_f}}^{\boldsymbol{apt}} L_{rn} + \boldsymbol{X}_{\boldsymbol{W}}^{\boldsymbol{max}} W_n \end{cases}. \tag{26}$$

Observing that the random load combination 1 is the same as the random load combination 3, the set of considered random load combinations can be simplified to

$$\begin{cases} 1: & \boldsymbol{X_D} D_n + \boldsymbol{X}_{\boldsymbol{L_f}}^{\boldsymbol{apt}} L_{fn} + \boldsymbol{X}_{\boldsymbol{L_f}}^{\boldsymbol{apt}} L_{rn} \\ 2: & \boldsymbol{X_D} D_n + \boldsymbol{X}_{\boldsymbol{L_f}}^{\boldsymbol{max}} L_{fn} + \boldsymbol{X}_{\boldsymbol{L_f}}^{\boldsymbol{max}} L_{rn} \\ 3: & \boldsymbol{X_D} D_n + \boldsymbol{X}_{\boldsymbol{L_f}}^{\boldsymbol{apt}} L_{fn} + \boldsymbol{X}_{\boldsymbol{L_f}}^{\boldsymbol{apt}} L_{rn} + \boldsymbol{X}_{\boldsymbol{W}}^{\boldsymbol{max}} W_n \end{cases}, \tag{27}$$

which was used to evaluate the system-level reliabilities of the optimal structural steel frame designs.

3.3 STATISTICS OF RANDOM VARIABLES

The statistics of the normalized random variables associated with loads are based on the statistics provided in Akchurin et al. (2024), which were assembled primarily from the early studies on the development of the LRFD and later studies on the updated provisions for the hazard-based wind loads (Ellingwood et al. 1982, 1980; Galambos et al. 1982; McAllister et al. 2018; ASCE 2021), while the statistics of the random variables representing the uncertainties present in the geometric and material properties of a structure are based on the statistics provided in Zhang et al. (2016a; b),

which were assembled primarily from comprehensive measurement studies on the variability of yield stresses, elastic moduli, cross-sectional dimensions, initial geometric imperfections, residual stresses of hot-rolled sections (Galambos and Ravindra 1978; Bartlett et al. 2003; Melcher et al. 2004; Shayan et al. 2014a; b), and are briefly described below.

3.3.1 RANDOM GEOMETRIC PROPERTIES

The random variable representing the initial frame out-of-plumbness imperfections $\boldsymbol{\psi}$ follows a lognormal distribution with mean μ of 1/770 and standard deviation σ of 1/880 (Shayan et al. 2014a). The initial member out-of-straightness imperfections were modeled as a linear combination of the first 3 randomly scaled buckling modes of a single column under compression $\boldsymbol{\delta}(x) = \sum_{m=1}^{3} \boldsymbol{a_m} \sin(\pi x/L)$ where x is the coordinate along the longitudinal axis of a structural member and $\boldsymbol{a_m}$ are normally distributed random scaling factors with a random sign, either positive or negative, for the m^{th} buckling mode (Zhang et al. 2016a; b). The statistics of the randoms scaling factors are provided in Table 1. Lastly, the variations in the cross-sectional dimensions of each structural member were considered in the system reliability analyses (Melcher et al. 2004). The statistics of the random variables associated with the cross-sectional dimensions of W-shaped sections are provided in Table 2 with the correlation matrix provided in Table 3. The geometric uncertainties were assigned to each structural member individually.

3.3.2 RANDOM MATERIAL PROPERTIES

In the system reliability analysis, the material assigned to the structural members was modeled using elastic-perfectly plastic constitutive model with the normalized random variable associated with the elastic modulus $\boldsymbol{X_E}$ following a normal distribution with a mean μ of 1.00 and a coefficient of variation V of 0.06, and the normalized random variable associated with the yield stress $\boldsymbol{X_{F_y}}$ following a lognormal distribution with μ of 1.05 and V of 0.10 (Galambos and Ravindra 1978; Bartlett et al. 2003). In the conducted system reliability analyses, it was assumed that the material properties of all structural members were perfectly correlated. However, the ECCS residual stress pattern used for each structural member was individually scaled by a normally distributed random scaling factor $\boldsymbol{\chi}$ with μ of 1.05 and V of 0.21 (Shayan et al. 2014b).

3.3.3 RANDOM LOADS

The normalized random variable associated with the dead load $\boldsymbol{X_D}$ follows a normal distribution with μ of 1.05 and V of 0.10. The normalized random variable associated with the arbitrary point-in-time floor live load $\boldsymbol{X_{L_f}^{apt}}$ follows a Gamma distribution with μ of 0.22 and V of 0.54. The normalized random variable associated with the maximum lifetime floor live load $\boldsymbol{X_{L_f}^{max}}$ follows a Gumbel distribution with μ of 1.10 and V of 0.19. Lastly, the normalized

random variable associated with the maximum lifetime floor live load $\boldsymbol{X_W^{max}}$ follows a Gumbel distribution with μ of 0.47 and V of 0.35 (Akchurin et al. 2024).

3.4 IMPORTANCE SAMPLING

To study the system-level reliabilities achieved by the design methods of interest for the benchmark structural steel frames, we employ *Importance Sampling* (IS), a Monte Carlo-based variance reduction technique widely adopted in structural and system reliability analysis (Melchers 1989; Ibrahim 1991; Buonopane and Schafer 2006), which improves the efficiency of probability of failure estimation by biasing samples towards the failure domain, thereby enabling accurate evaluation of small probabilities of failure with a significantly reduced number of samples compared to brute-force Monte Carlo simulation. In the following sections, we give a brief overview of the derivation of the numerical IS estimators for the system-level probability of failure P_f and the corresponding generalized system-level reliability index β.

The system-level probability of failure P_f is given by the integral of the joint probability density function (PDF) $f_{\vec{\boldsymbol{X}}}(\vec{x})$ of the random variables $\vec{\boldsymbol{X}}$ over the failure domain $\mathcal{F}_{\vec{\boldsymbol{X}}} = \{\vec{x}: G(\vec{x}) \leq 0\}$, such that

$$P_f = \int_{\mathcal{F}_{\vec{\boldsymbol{X}}}} f_{\vec{\boldsymbol{X}}}(\vec{x}) d\vec{x}, \tag{28}$$

which is conventionally converted from the space of physical random variables $\vec{\boldsymbol{X}}$ into the space of uncorrelated standard normal random variables $\vec{\boldsymbol{U}}$ through an isoprobabilistic transformation $\vec{\boldsymbol{U}} = T(\vec{\boldsymbol{X}})$. The Generalized Nataf Transformation (Nataf 1962; Lebrun and Dutfoy 2009a; b) is employed in this study, for the purpose of simplifying the development of a robust *proposal density function* $q(\vec{u})$, which is used to bias samples towards the failure domain. Applying this transformation, the system-level probability of failure P_f in Eq. (28) is now given by the integral of the joint PDF $\phi(\vec{u})$ of the uncorrelated standard normal random variables $\vec{U}$, which is known analytically, over the failure domain $\mathcal{F}_{\vec{\boldsymbol{U}}} = \{\vec{u}: G(\vec{x} = T(\vec{u})) \leq 0\}$, such that

$$P_f = \int_{\mathcal{F}_{\vec{U}}} \phi(\vec{u}) d\vec{u}. \tag{29}$$

Since the failure domain $\mathcal{F}_{\vec{\boldsymbol{U}}}$ in the standard normal space is not known analytically, as it is a result of the nonlinear transformation $\vec{\boldsymbol{U}} = T(\vec{\boldsymbol{X}})$ of the failure domain $\mathcal{F}_{\vec{\boldsymbol{X}}}$ in the physical space, which itself a result of the 2nd-order inelastic analysis, it is useful to introduce an indicator function $\mathbb{I}(\vec{u})$ equal to 1 if the sample $\vec{u}$ falls within the failure domain $\mathcal{F}_{\vec{\boldsymbol{U}}}$, such that $G(\vec{x} = T(\vec{u})) \leq 0$, and 0 otherwise to allow integration over the entire standard normal space. Introducing the indicator function $\mathbb{I}(\vec{u})$ and the proposal density function $q(\vec{u})$ into Eq. (29), we find that the system-

level probability of failure P_f is given by the expectation of $\mathbb{I}(\vec{\boldsymbol{U}})\phi(\vec{\boldsymbol{U}})/q(\vec{\boldsymbol{U}})$ with respect to the proposal density function $q(\vec{u})$, such that

$$P_f = \int_{\mathbb{R}^{N_{\mathrm{RV}}}} \mathbb{I}(\vec{u})\phi(\vec{u})d\vec{u} = \int_{\mathbb{R}^{N_{\mathrm{RV}}}} \frac{\mathbb{I}(\vec{u})\phi(\vec{u})}{q(\vec{u})} q(\vec{u})d\vec{u} = \mathbb{E}_q\left[\frac{\mathbb{I}(\vec{\boldsymbol{U}})\phi(\vec{\boldsymbol{U}})}{q(\vec{\boldsymbol{U}})}\right]. \tag{30}$$

Thus, the numerical IS estimator for the system-level probability of failure P_f is given by

$$\tilde{P}_f = \frac{1}{N_{\mathrm{S}}}\sum_{i=1}^{N_{\mathrm{S}}} \frac{\mathbb{I}(\vec{u}_i)\phi(\vec{u}_i)}{q(\vec{u}_i)}, \tag{31}$$

where N_{S} is the number of samples $\vec{u}_i$ generated from the proposal density function $q(\vec{u})$. The numerical IS estimator for the corresponding generalized system-level reliability index β, which serves as a more familiar measure of reliability, is given by

$$\tilde{\beta} = -\Phi^{-1}(\tilde{P}_f). \tag{32}$$

In the IS, the choice of the proposal density function $q(\vec{u})$ is crucial to ensure variance reduction of the numerical IS estimators for P_f and β. As discussed in Der Kiureghian (2022), a robust choice for the proposal density function $q(\vec{u})$ for limit state functions for series systems, such as the one given by Eq. (22), is a Gaussian mixture model with multivariate standard normal components $\phi(\vec{u})$ centered at the design points $\vec{u} = \vec{u}_i^*$ of each limit state function $g_i(\vec{\boldsymbol{X}})$ for each random load combination i, which can be obtained using the first-order reliability method (FORM), such that

$$q(\vec{u}) = \sum_{i=1}^{N_{\mathrm{RLC}}} w_i \phi(\vec{u} - \vec{u}_i^*), \tag{33}$$

where w_i are the weights assigned to each component of the Gaussian mixture model satisfying the condition $\sum_{i=1}^{N_{\mathrm{RLC}}} w_i = 1$, which ensures its correct normalization. The purpose of centering the components at the design points in Eq. (33) is to maximize the number of samples in the failure domain $\mathcal{F}_{\vec{\boldsymbol{U}}}$. The weights w_i for the Gaussian components are set to be inversely proportional to the norms of the vectors to the design points to maximize the number of samples drawn in the regions of the failure domain $\mathcal{F}_{\vec{\boldsymbol{U}}}$ with more probability content, such that $w_i \propto 1/|\vec{u}_i^*|$. Using these weights, we arrive at the following formulation of the proposal density function used to estimate P_f in Eq. (31) and the corresponding β in Eq. (32):

$$q(\vec{u}) = \frac{\sum_{i=1}^{N_{\mathrm{RLC}}} \phi(\vec{u} - \vec{u}_i^*)/|\vec{u}_i^*|}{\sum_{i=1}^{N_{\mathrm{RLC}}} 1/|\vec{u}_i^*|}. \tag{34}$$

3.5 PROCEDURE

For each structural steel frame design, the system reliability analysis is conducted using the following procedure: (1) FORM was performed using the improved Hasofer-Lind-Rackwitz-Fiessler method (Der Kiureghian 2022; Liu and Der Kiureghian 1986) to find the design points $\vec{u}_i^*$ of each limit state function $g_i(\vec{\boldsymbol{X}})$ for each random load combination

i, (2) the proposal density function $q(\vec{u})$ in Eq. (34) was constructed, (3) $N_S = 10{,}000$ samples were generated from $q(\vec{u})$ using Latin Hypercube Sampling for further variance reduction of the numerical estimators, (4) P_f was evaluated using Eq. (31) by performing N_S 2nd-order inelastic analyses of the structural steel frame design, and, lastly, (5) the corresponding β was evaluated from Eq. (32). Each step of the procedure was carried out using the `Fortuna.jl` package, an open-source Julia package for structural and system reliability analysis (Akchurin 2024).

4 RESULTS

4.1 RESULTS OF STRUCTURAL DESIGN OPTIMIZATION

The structural design optimization framework successfully identified optimal designs for all 22 benchmark structural steel frames according to each design method using both proportional and nonproportional loadings, which are provided in Supplementary Materials. To facilitate comparison, weight ratios relative to the designs obtained using the DAM, calculated for designs obtained using either proportional or nonproportional loading, are presented in Fig. 3 and tabulated in Table 4. Normalizing against the DAM is appropriate, as the DAM represents the most commonly used design method in U.S. practice, making these comparisons meaningful for structural engineers and highlighting the potential advantages of system-based design methods. Fig. 3 demonstrates that system-based design methods – AIAM, DDM90, and DDM85 – consistently produce substantially lighter structural designs compared to the component-based methods – DAM and AEAM – regardless of whether proportional or nonproportional loading is used during the design process with average weight reductions of 16.1(PL)/16.7(NL)% for the AIAM, 13.4/14.7% for the DDM85 and 16.3/16.9% for the DDM90 when compared to the DAM. The corresponding maximum weight reductions are 28.3/32.3% for the AIAM, 30.9/31.1% for the DDM85, and 32.1%/31.5% for the DDM90. In general, the DAM and AEAM design methods result in nearly identical weights for all frames, while the AIAM and DDM90 result in the lightest designs, closely followed by DDM85, which is only slightly heavier. These trends remain consistent across all benchmark structural steel frames, indicating that the weight reduction benefits of system-based design methods are robust to variations in structural configurations and loading conditions.

The comparison of the weights of the optimal designs obtained using proportional and nonproportional loadings, presented in Fig. 4, demonstrates that, for the component-based design methods, there is minimal difference in the resulting weights between the two types of loadings, indicating that these design methods are relatively insensitive to how the loads are applied during the design process. In contrast, for the system-based design methods, using nonproportional loading can lead to modestly lighter designs compared to proportional loading in some cases, though,

on average, the difference remains relatively small across all of the analyzed structural steel frames: 1.1% for the AIAM, 1.8% for the DDM85, and 1.0% for the DDM90.

4.2 Results of System Reliability Analysis

Performing the system reliability analyses that included uncertainties in geometric properties, material properties, and applied loads using the Importance Sampling technique for each optimal structural steel frame design, the system-level reliability indices β presented in Table 5 were obtained. These values of β provide a robust quantitative basis for comparing the system-level reliabilities achieved by the design methods of interest relative to each other and the target levels of reliability specified in design codes. For example, a target reliability index β_t of 3.0 is recommended in the ASCE 7-22 Standard for Risk Category II buildings utilizing performance-based design procedures (Table 1.3-1). The structural member strength provisions of the AISC 360-22 Specification generally targeted β_t of 3.0, but allowed values as low as 2.6, while the provisions of the AISI S100-24 Specification (ANSI/SDI 2024) were calibrated to β_t of 2.5 for members and 3.5 for connections. For comparison purposes, system-level target reliabilities β_t of 2.5 and 3.0 are highlighted herein. Final selection of target levels of system reliability requires input from design code committees and professionals.

To facilitate comparison, β values of the optimal designs obtained according to the requirements of each design method of interest are presented in Fig. 5. The component-based design methods – DAM and AEAM – result in β values that exceed β_t of 3.0 for 20 out of 22 frames for the DAM and 18 out of 22 frames for the AEAM, reflecting a conservative margin in reliability as they ensure reliability on the level of individual structural components without consideration of the potential for significant force redistribution as a system or its significant portion reaches a strength limit state. In contrast, the system-based design methods – AIAM and DDM – overall result in β values that fall closer to β_t of 3.0. This trend is evident from the mean β values reported in Table 5, which range from 2.8 to 3.1, as well as from the substantially reduced variability, with V decreasing from 18.7-20.6% for the component-based design methods to 7.9-10.4% for the system-based design methods. This highlights the efficiency of system-based design methods in material utilization while also emphasizing the need for careful calibration to ensure that target levels of reliability are consistently met.

The comparison between β values of the optimal designs obtained using proportional and nonproportional loadings, is presented in Fig. 6, demonstrates that the designs obtained using proportional loading are more reliable than the

designs obtained using nonproportional loading, especially for the system-based design methods, which is consistent with the fact that system-based design methods result in lighter designs as observed in Fig. 4.

5 SENSITIVITY OF ADVANCED INELASTIC ANALYSIS METHOD

As observed in Fig. 5, the AIAM with the reduction factor of 0.90 for E and F_y as currently specified in Appendix 1 of the AISC 360-22 Specification, referred to as the AIAM90, consistently resulted in β values around 2.85. To understand the sensitivity of the design method to the selected reductions we considered a modest recalibration of the reduction factor, through an additional set of optimal designs obtained according to the AIAM, but with a more conservative reduction factor on E and F_y of 0.85, referred to as AIAM85. The resulting weights and system-level reliability indices of the optimal designs are presented in Table 6.

Comparing β values between the AIAM85 and AIAM90, shown in Fig. 7, we can observe that using the reduction factor of 0.85 leads to an increase in β values, as reflected by an increase in the mean β values from 2.85 (Table 5) to 3.15 (Table 6) – this represents a roughly threefold reduction in the mean P_f values from 2.2×10^{-3} to 8.2×10^{-4}. This change is achieved at the cost of slightly heavier designs, with an average weight increase of 3.4%, as shown in Fig. 8, when compared to the AIAM90. When compared to the DAM, AIAM90 provides weight savings of 16.1/16.7% and AIAM85 provides weight savings of 13.3/14.0%. Overall, this sensitivity exercise demonstrates that modest changes in the reduction factor can have robust changes on the system-level reliability while still maintaining material efficiency.

6 DISCUSSION

This study examines system-level reliabilities achieved by two component-based design methods and two system-based design methods for a series of benchmark structural steel frames using a combined framework of structural design optimization and system reliability analysis. The results demonstrate clear and systematic differences between the two categories of design methods in terms of achieved reliability, variability, and material efficiency.

The component-based design methods – DAM and AEAM – consistently produced designs with β values exceeding β_t of 3.0, with mean β values ranging between 3.7 and 3.8, and high variability as reflected by V values ranging from 18.7 to 20.6%. This trend reflects the inherently conservative nature of component-based design, in which reliability is enforced at the level of first individual structural members, and the potential for inelastic force redistribution is not accounted for. In contrast, the system-based design methods – AIAM and DDM – produced significantly lighter designs, highlighting their material and economic efficiency, with β values that were generally closer to β_t of 3.0 and

exhibited substantially lower variability; for these design methods, mean β values ranged between 2.8 and 3.1, with V values ranging from 7.9 to 10.4%. The low variability reflects more consistent system-level reliability outcomes enabled by explicit consideration of beneficial inelastic load redistribution effects. These improvements in system-level reliabilities are accompanied by significant reductions in structural weight. Relative to the DAM, the average weight reduction of 16.1/16.7% was achieved for the AIAM, 13.4/14.7% for the DDM85 and 16.3/16.9% for the DDM90. In conclusion, these results demonstrate that system-based design methods achieve lower structural weights not by sacrificing safety, but by allocating material more efficiently at the system level, thereby reducing excess conservatism inherent in component-based design methods.

The results also indicate that, similar to DDM90, the system-level reliabilities of AIAM designs, when implemented using the reduction factor of 0.90 specified in Appendix 1 of the AISC 360-22 Specification (AIAM90), frequently fall below β_t of 3.0. This observation motivated a modest sensitivity study of the AIAM's reduction factor. Using a reduction factor of 0.85 (AIAM85) resulted in an increase in the mean β values from approximately 2.85 to 3.15. This improvement was achieved with a modest average weight increase of only 3.4% relative to AIAM90. Despite this increase, AIAM85 designs remain substantially more materially efficient than component-based designs, retaining weight reductions of 13.3/14.0% relative to DAM, compared to 16.1/16.7% for AIAM90. These results demonstrate that a modest changes in the reduction factor can have robust changes on the system-level reliability while largely preserving significant weight reduction benefits.

To conclude, the findings of this study demonstrate a clear trade-off between the weight of a structure and its system-level reliability. System-based design methods offer a path towards more materially efficient designs of structural steel buildings by capturing, although complex, beneficial inelastic load redistribution effects omitted in component-based methods. However, this advantage comes with the caveat that these design methods require careful calibration of the embedded reduction factors to achieve adequate levels of safety.

This study is limited to planar structural steel frames with compact W-shaped sections, which may impact the generalizability of findings to other structural archetypes, non-compact sections, and spatial structures. Additionally, simplifications such as treating roof live loads as floor live loads may affect the accuracy of the system reliability analysis. The present study also considers only peak strength as the governing system-level limit state and other system-level limit states related to serviceability could be examined in future work. However, strength-based limit states align most directly with the system reliability analysis formulations adopted here, in a manner consistent with

component-based design methods where limit states are commonly expressed in terms of strength-based limit state functions.

7 CONCLUSION

In this study, a clear generic framework for evaluating the system-level reliability of arbitrary steel structures designed using any arbitrary design method was developed. The framework is based on the use of a structural design optimization framework employing the Genetic Algorithm to identify optimal designs with least possible weights, combined with a robust system reliability analysis employing the Importance Sampling technique to account for uncertainties in geometric properties, material properties, and applied loads to accurately evaluate the system-level reliabilities.

Applying this framework to the benchmark structural steel frames of interest, the study demonstrates that system-based design methods enable the development of lighter and more efficient steel structures compared to traditional component-based design methods, though careful calibration is essential to ensure that adequate levels of safety are always achieved. By systematically analyzing structural weights and system-level reliabilities across the representative structural steel frames, the study provides evidence that modest adjustments to reduction factors can align system-based design methods' safety with design code requirements while preserving material efficiency. These results support the continued advancement and broader adoption of system-based design methods in future design codes for structural steel buildings.

DATA AVAILABILITY STATEMENT

Some or all data, models, or code that support the findings of this study are available from the corresponding author upon reasonable request.

ACKNOWLEDGEMENTS

The authors would like to thank the American Institute of Steel Construction for the financial support of the "*System Reliability of Steel Structures*" project. The authors would also like to thank Dr. Jesús-Adolfo Mejía-de-Dios and Dr. Efrén Mezura-Montes from the University of Veracruz for developing the `Metaheuristics.jl` package and providing invaluable support in its application. The first author would also like to personally thank fellow graduate students Saroj Khanal and Tomás Tapia from the Johns Hopkins University for insightful discussions on the discrete optimization problems with nonlinear constraints. Lastly, the first author would also like to thank Kyurae Kim, a graduate student from the University of Pennsylvania, who provided valuable tips on generating samples from

Gaussian mixture models using the Latin Hypercube Sampling technique and improving the stability of the implementation of the Generalized Nataf Transformation in the `Fortuna.jl` package.

SUPPLEMENTARY MATERIALS

The supplementary materials are available at the following URL:
https://archive.data.jhu.edu/dataset.xhtml?persistentId=doi:10.7281/T1OH6BUP&version=DRAFT.

REFERENCES

AISC. 1923. *AISC: Standard Specification*. American Institute of Steel Construction. American Institute of Steel Construction.

AISC. 1967. *AISC: Manual of Steel Construction*. American Institute of Steel Construction. American Institute of Steel Construction.

AISC. 1986. *AISC: Load and Resistance Factor Design Specification for Structural Steel Buildings*. American Institute of Steel Construction. American Institute of Steel Construction.

AISC. 2005. *ANSI/AISC 360-05: Specification for Structural Steel Buildings*. American Institute of Steel Construction. American Institute of Steel Construction.

AISC. 2010. *ANSI/AISC 360-10: Specification for Structural Steel Buildings*. American Institute of Steel Construction. American Institute of Steel Construction.

AISC. 2016. *ANSI/AISC 360-16: Specification for Structural Steel Buildings*. American Institute of Steel Construction. American Institute of Steel Construction.

AISC. 2022. *ANSI/AISC 360-22: Specification for Structural Steel Buildings*. American Institute of Steel Construction. American Institute of Steel Construction.

AISC. 2023. *AISC: Steel Construction Manual*. American Institute of Steel Construction. Chicago, Illinois: American Institute of Steel Construction.

Akchurin, D. 2024. "Fortuna.jl: Structural and System Reliability Analysis in Julia." *Journal of Open Source Software*, 9 (100): 6967. https://doi.org/10.21105/joss.06967.

Akchurin, D., S. Ádány, R. D. Ziemian, K. J. R. Rasmussen, and B. W. Schafer. 2025. "System-Based Design Methods: Stability and Reliability of Benchmark Structural Steel Frames." In: *Proceedings of the Annual Stability Conference*. Louisville, KY: Structural Stability Research Council.

Akchurin, D., R. Sabelli, R. D. Ziemian, and B. W. Schafer. 2024. "ASD and LRFD: Reliability Comparison for Designs Subjected to Wind Loads." *Journal of Constructional Steel Research*, 213: 108327. https://doi.org/10.1016/j.jcsr.2023.108327.

ANSI/SDI. 2024. *ANSI/SDI AISI S100-2024: North American Specification for the Design of Cold-Formed Steel Structural Members*. Steel Deck Institute. Steel Deck Institute.

Arrayago, I., and K. J. R. Rasmussen. 2022. "Reliability of Stainless Steel Frames Designed Using the Direct Design Method in Serviceability Limit States." *Journal of Constructional Steel Research*, 196: 107425. https://doi.org/10.1016/j.jcsr.2022.107425.

Arrayago, I., K. J. R. Rasmussen, and H. Zhang. 2022. "System-Based Reliability Analysis of Stainless Steel Frames Subjected to Gravity and Wind Loads." *Structural Safety*, 97: 102211. https://doi.org/10.1016/j.strusafe.2022.102211.

ASCE. 2021. *ASCE 7-22: Minimum Design Loads and Associated Criteria for Buildings and Other Structures*. American Society of Civil Engineers. American Society of Civil Engineers.

Bartlett, F. M., R. J. Dexter, M. D. Graeser, J. J. Jelinek, B. J. Schmidt, and T. V. Galambos. 2003. "Updating Standard Shape Material Properties Database for Design and Reliability." *Engineering Journal*, 40 (1): 2–14. https://doi.org/10.62913/engj.v40i1.800.

Beedle, L. S. 1970. *Plastic Design of Steel Frames*. New York: Wiley.

Buonopane, S. G., and B. W. Schafer. 2006. "Reliability of Steel Frames Designed with Advanced Analysis." *Journal of Structural Engineering*, 132 (2): 267–276. https://doi.org/10.1061/(ASCE)0733-9445(2006)132:2(267).

Deb, K. 2000. "An Efficient Constraint Handling Method for Genetic Algorithms." *Computer Methods in Applied Mechanics and Engineering*, 186 (2–4): 311–338. https://doi.org/10.1016/S0045-7825(99)00389-8.

Deb, K., and R. B. Agrawal. 1995. "Simulated Binary Crossover for Continuous Search Space." *Complex Systems*, 9: 115–148.

Deb, K., and A. Deb. 2014. "Analysing Mutation Schemes for Real-Parameter Genetic Algorithms." *International Journal of Artificial Intelligence and Soft Computing*, 4 (1): 1. https://doi.org/10.1504/IJAISC.2014.059280.

Deierlein, G. G., J. F. Hajjar, J. A. Yura, D. W. White, and W. F. Baker. 2002. "Proposed New Provisions for Frame Stability Using Second-Order Analysis." In: *Proceedings of the Annual Stability Conference*. Seattle, WA: Structural Stability Research Council.

Der Kiureghian, A. 2022. *Structural and System Reliability*. Cambridge: Cambridge University Press.

Ellingwood, B., J. G. MacGregor, T. V. Galambos, and C. A. Cornell. 1982. "Probability Based Load Criteria: Load Factors and Load Combinations." *Journal of the Structural Division*, 108 (5): 978–997. https://doi.org/10.1061/JSDEAG.0005959.

Ellingwood, B. R., T. V. Galambos, J. G. MacGregor, and C. A. Cornell. 1980. *Development of a Probability Based Load Criterion for American National Standard A58, National Bureau of Standards*. Research Report. Washington, DC.
Galambos, T. V. 1981. "Load and Resistance Factor Design." *Engineering Journal*.
Galambos, T. V., B. Ellingwood, J. G. MacGregor, and C. A. Cornell. 1982. "Probability Based Load Criteria: Assessment of Current Design Practice." *Journal of the Structural Division*, 108 (5): 959–977. https://doi.org/10.1061/JSDEAG.0005958.
Galambos, T. V., and M. K. Ravindra. 1978. "Properties of Steel for Use in LRFD." *Journal of the Structural Division*, 104 (9): 1459–1468. https://doi.org/10.1061/JSDEAG.0004988.
Giensen Loo, E. J. 2016. "Design of Steel Structures by Advanced Second-Order Elastic Analysis: Background Studies." Bucknell University.
Goldberg, D. E. 2012. *Genetic Algorithms in Search, Optimization, and Machine Learning*. 30. print. Boston: Addison-Wesley.
Ibrahim, Y. 1991. "Observations on Applications of Importance Sampling in Structural Reliability Analysis." *Structural Safety*, 9 (4): 269–281. https://doi.org/10.1016/0167-4730(91)90049-F.
Karasu, A., K. D. Peterman, and S. R. Arwade. 2022. "Analysis of Roof Live Loads in Industrial Buildings." In: *Proceedings of the Cold-Formed Steel Research Consortium Colloquium*.
Karasu, A., K. D. Peterman, and S. R. Arwade. 2025. "Roof Live Loads for Low-Slope Roofs." *Journal of Structural Engineering*, 151 (6): 04025064. https://doi.org/10.1061/JSENDH.STENG-14363.
Lebrun, R., and A. Dutfoy. 2009a. "A Generalization of the Nataf Transformation to Distributions with Elliptical Copula." *Probabilistic Engineering Mechanics*, 24 (2): 172–178. https://doi.org/10.1016/j.probengmech.2008.05.001.
Lebrun, R., and A. Dutfoy. 2009b. "An Innovating Analysis of the Nataf Transformation from the Copula Viewpoint." *Probabilistic Engineering Mechanics*, 24 (3): 312–320. https://doi.org/10.1016/j.probengmech.2008.08.001.
Liu, H. 2019. "System Reliability Calibrations for the Direct Design Method of Planar Steel Frames with Partially Restrained Connections." University of Sydney.
Liu, P.-L., and A. Der Kiureghian. 1986. *Optimization Algorithms for Structural Reliability Analysis*. SEMM Reports Series. Research Report. Berkley, CA: University of California Berkley.
Liu, W. 2016. "System Reliability-Based Design of Three-Dimensional Steel Structures by Advanced Analysis." University of Sydney.
Liu, W., H. Zhang, K. J. R. Rasmussen, and S. Yan. 2019. "System-Based Limit State Design Criterion for 3D Steel Frames Under Wind Loads." *Journal of Constructional Steel Research*, 157: 440–449. https://doi.org/10.1016/j.jcsr.2019.02.015.
Maleck, A. E. 2001. "Second-Order Inelastic and Modified Elastic Analysis and Design Evaluation of Planar Steel Frames." Georgia Institute of Technology.
Maleck, A. E., and D. W. White. 2003. "Direct Analysis Approach for the Assessment of Frame Stability: Verification Studies." In: *Proceedings of the Annual Stability Conference*. Baltimore, MD: Structural Stability Research Council.
Martinez-Garcia, J. M. 2002. "Benchmark Studies to Evaluate New Provisions for Frame Stability Using Second-Order Analysis." Bucknell University.
Martinez-Garcia, J. M., and R. D. Ziemian. 2006. "Benchmark Studies to Compare Frame Stability Provisions." In: *Proceedings of the Annual Stability Conference*. San Antonio, TX: Structural Stability Research Council.
McAllister, T. P., N. Wang, and B. R. Ellingwood. 2018. "Risk-Informed Mean Recurrence Intervals for Updated Wind Maps in ASCE 7-16." *Journal of Structural Engineering*, 144 (5): 06018001. https://doi.org/10.1061/(ASCE)ST.1943-541X.0002011.
McAllister, T., R. Zheng Guo, and J. Y. Lee, eds. 2025. *Structural Reliability Guidance in ASCE 7-22: Principles and Methods*. Reston, VA: American Society of Civil Engineers.
McKenna, F., M. H. Scott, and G. L. Fenves. 2010. "Nonlinear Finite-Element Analysis Software Architecture Using Object Composition." *Journal of Computing in Civil Engineering*, 24 (1): 95–107. https://doi.org/10.1061/(ASCE)CP.1943-5487.0000002.
Mejía-de-Dios, J.-A., and E. Mezura-Montes. 2022. "Metaheuristics.jl: A Julia Package for Single- and Multi-Objective Optimization." *Journal of Open Source Software*, 7 (78): 4723. https://doi.org/10.21105/joss.04723.
Melcher, J., Z. Kala, M. Holický, M. Fajkus, and L. Rozlívka. 2004. "Design Characteristics of Structural Steels Based on Statistical Analysis of Metallurgical Products." *Journal of Constructional Steel Research*, 60 (3–5): 795–808. https://doi.org/10.1016/S0143-974X(03)00144-5.
Melchers, R. E. 1989. "Importance Sampling in Structural Systems." *Structural Safety*, 6 (1): 3–10. https://doi.org/10.1016/0167-4730(89)90003-9.
Nataf, A. 1962. "Étude Graphique De Détermination De Distributions De Probabilités Planes Dont Les Marges Sont Données." *Comptes Rendus de l'Académie des Sciences*, 225: 42–43.
Nwe Nwe, M. T. 2014. "The Modified Direct Analysis Method: An Extension of the Direct Analysis Method." Bucknell University.
Shayan, S. 2013. "System Reliability-Based Design of 2D Steel Frames by Advanced Analysis." University of Sydney.
Shayan, S., K. J. R. Rasmussen, and H. Zhang. 2014a. "On the Modelling of Initial Geometric Imperfections of Steel Frames in Advanced Analysis." *Journal of Constructional Steel Research*, 98: 167–177. https://doi.org/10.1016/j.jcsr.2014.02.016.

Shayan, S., K. J. R. Rasmussen, and H. Zhang. 2014b. “Probabilistic Modelling of Residual Stress in Advanced Analysis of Steel Structures.” *Journal of Constructional Steel Research*, 101: 407–414. https://doi.org/10.1016/j.jcsr.2014.05.028.
Standards Australia. 2002a. *AS/NZS 1170.0 - Structural Design Actions, Part 0: General Principles*. Standards Australia. Sydney, Australia: Standards Australia.
Standards Australia. 2002b. *AS/NZS 1170.1 - Structural Design Actions, Part 1: Permanent, Imposed and Other Actions*. Standards Australia. Sydney, Australia: Standards Australia.
Standards Australia. 2018. *AS/NZS 4600 - Cold-Formed Steel Structures*. Standards Australia. Sydney, Australia: Standards Australia.
Standards Australia. 2023a. *AS/NZS 4084.1 - Steel Storage Racking, Part 1: Design*. Standards Australia. Sydney, Australia: Standards Australia.
Standards Australia. 2023b. *AS/NZS 3610.2 - Formwork for Concrete, Part 2: Design and Construction*. Standards Australia. Sydney, Australia: Standards Australia.
Surovek-Maleck, A. E., and D. W. White. 2004a. “Alternative Approaches for Elastic Analysis and Design of Steel Frames. I: Overview.” *Journal of Structural Engineering*, 130 (8): 1186–1196. https://doi.org/10.1061/(ASCE)0733-9445(2004)130:8(1186).
Surovek-Maleck, A. E., and D. W. White. 2004b. “Alternative Approaches for Elastic Analysis and Design of Steel Frames. II: Verification Studies.” *Journal of Structural Engineering*, 130 (8): 1197–1205. https://doi.org/10.1061/(ASCE)0733-9445(2004)130:8(1197).
Turkstra, C. J., and H. O. Madsen. 1980. “Load Combinations in Codified Structural Design.” *Journal of the Structural Division*, 106 (12): 2527–2543. https://doi.org/10.1061/JSDEAG.0005599.
Wang, Y., and R. D. Ziemian. 2019. “Design by Advanced Elastic Analysis: An Investigation of Beam-Columns Resisting Minor-Axis Bending.” In: *Proceedings of the Annual Stability Conference*. St. Louis, MO: Structural Stability Research Council.
Wang, Y., and R. D. Ziemian. 2021. “Design by Advanced Elastic Analysis: An Investigation of Beam-Columns.” *Engineering Journal*, 58 (2): 123–137. https://doi.org/10.62913/engj.v58i2.1174.
Yan, S., and K. J. R. Rasmussen. 2021. “Generalised Component Method-Based Finite Element Analysis of Steel Frames.” *Journal of Constructional Steel Research*, 187: 106949. https://doi.org/10.1016/j.jcsr.2021.106949.
Zhang, H., H. Liu, B. R. Ellingwood, and K. J. R. Rasmussen. 2018. “System Reliabilities of Planar Gravity Steel Frames Designed by the Inelastic Method in AISC 360-10.” *Journal of Structural Engineering*, 144 (3): 04018011. https://doi.org/10.1061/(ASCE)ST.1943-541X.0001991.
Zhang, H., S. Shayan, K. J. R. Rasmussen, and B. R. Ellingwood. 2016a. “System-Based Design of Planar Steel Frames, I: Reliability Framework.” *Journal of Constructional Steel Research*, 123: 135–143. https://doi.org/10.1016/j.jcsr.2016.05.004.
Zhang, H., S. Shayan, K. J. R. Rasmussen, and B. R. Ellingwood. 2016b. “System-Based Design of Planar Steel Frames, II: Reliability Results and Design Recommendations.” *Journal of Constructional Steel Research*, 123: 154–161. https://doi.org/10.1016/j.jcsr.2016.05.005.
Zhu, C., K. J. R. Rasmussen, and S. Yan. 2019. “Generalised Component Model for Structural Steel Joints.” *Journal of Constructional Steel Research*, 153: 330–342. https://doi.org/10.1016/j.jcsr.2018.10.026.
Ziemian, C. W., and R. D. Ziemian. 2021. “Efficient Geometric Nonlinear Elastic Analysis for Design of Steel Structures: Benchmark Studies.” *Journal of Constructional Steel Research*, 186: 106870. https://doi.org/10.1016/j.jcsr.2021.106870.
Ziemian, R. D., W. McGuire, and G. G. Deierlein. 1992a. “Inelastic Limit States Design. Part I: Planar Frame Studies.” *Journal of Structural Engineering*, 118 (9): 2532–2549. https://doi.org/10.1061/(ASCE)0733-9445(1992)118:9(2532).
Ziemian, R. D., W. McGuire, and G. G. Dierlein. 1992b. “Inelastic Limit States Design Part II: Three-Dimensional Frame Study.” *Journal of Structural Engineering*, 118 (9): 2550–2568. https://doi.org/10.1061/(ASCE)0733-9445(1992)118:9(2550).

FIGURES

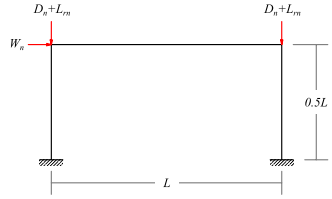

Frame #1
L = 9,144 mm (30’)
$\psi = 1/500$ (rightward)

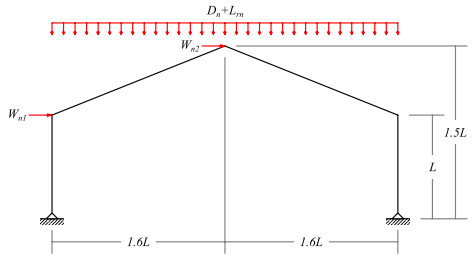

Frame #2
L = 7,620 mm (25’)
$\psi = 1/500$ (rightward)

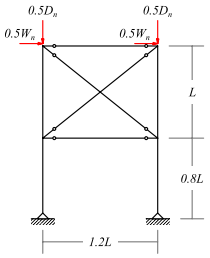

Frame #3
L = 3,048 mm (10’)
$\psi = 1/500$ (rightward)

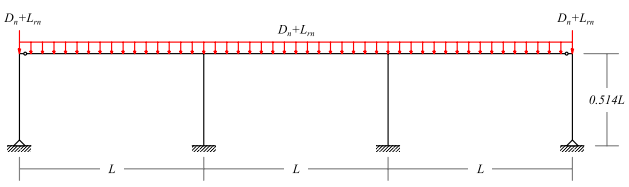

Frame #4
L = 10,688 mm (35’)
$\psi = 1/500$ (rightward)

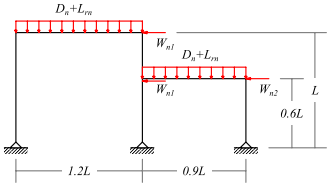

Frame #5
L = 6,069 mm (20’)
$\psi = 1/500$ (leftward)

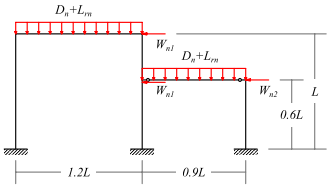

Frame #6
L = 6,069 mm (20’)
$\psi = 1/500$ (leftward)

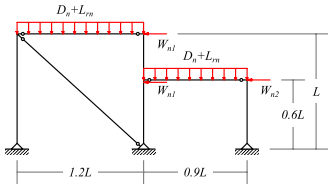

Frame #7
L = 6,069 mm (20’)
$\psi = 1/500$ (leftward)

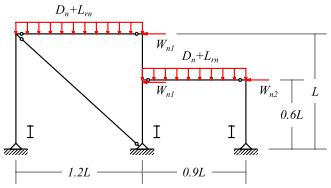

Frame #8
L = 6,069 mm (20’)
$\psi = 1/500$ (leftward)

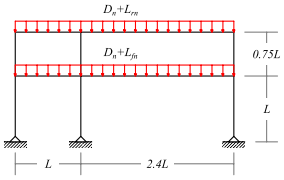

Frame #9
L = 6,069 mm (20’)
$\psi = 1/500$ (leftward)

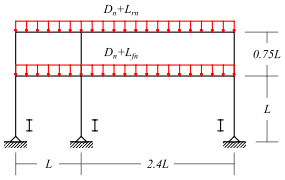

Frame #10
L = 6,069 mm (20’)
$\psi = 1/500$ (leftward)

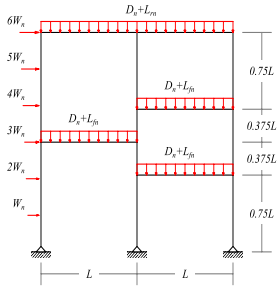

Frame #11
L = 6,069 mm (20’)
$\psi = 1/500$ (rightward)

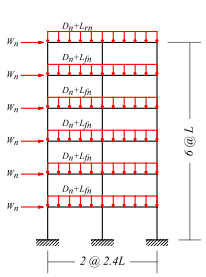

Frame #12
L = 3,750 mm (12.3’)
$\psi = 1/500$ (rightward)

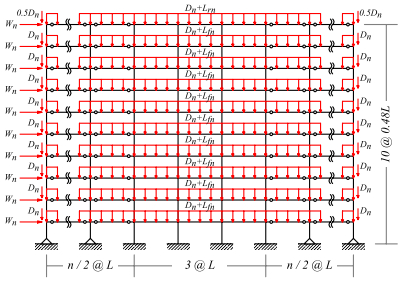

Frames #13 to #16
L = 6,069 mm (20’)
$\psi = 1/500$ (rightward)
n = {0, 4, 8, 12} lean-on columns

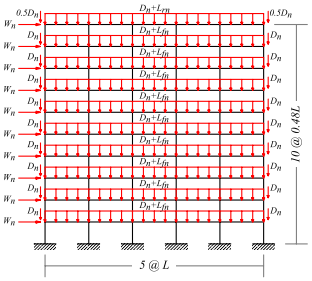

Frame #17
L = 6,069 mm (20’)
$\psi = 1/500$ (rightward)

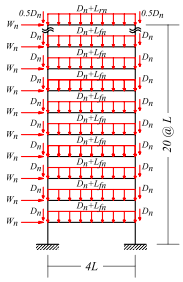

Frame #18
L = 4,267 mm (14’)
$\psi = 1/500$ (rightward)

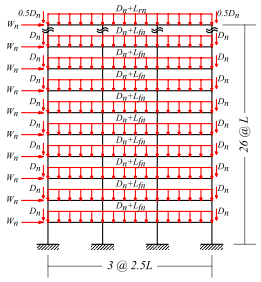

Frame #19
L = 3,658 mm (12’)
$\psi = 1/500$ (rightward)

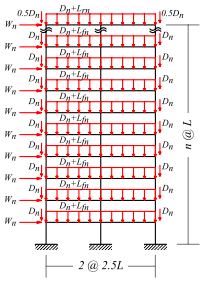

Frames #20 to #22
L = 3,658 mm (12’)
$\psi = 1/500$ (rightward)
n = {30, 30, 40} stories

Fig. 1: Benchmark structural steel frames.

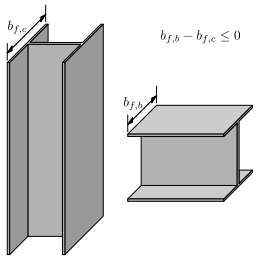

(a) Beam-to-column connections: Column bending about major axis

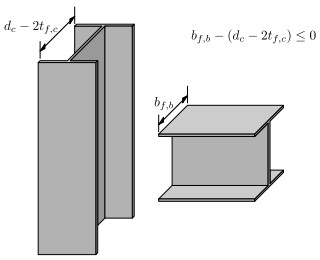

(b) Beam-to-column connections: Column bending about minor axis

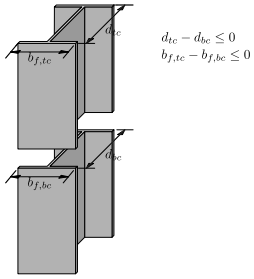

(c) Column-to-column connections

Fig. 2: Constructability constraints.

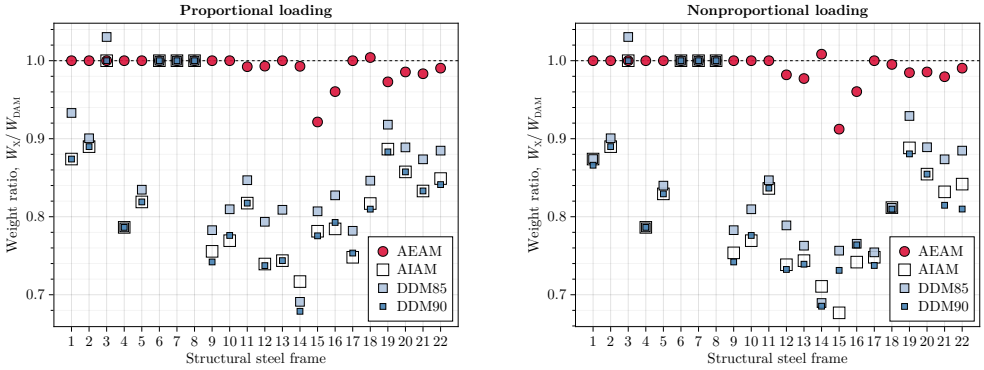

Fig. 3: Weights ratios between the optimal designs obtained using the design methods of interest and the optimal designs obtained using the DAM.

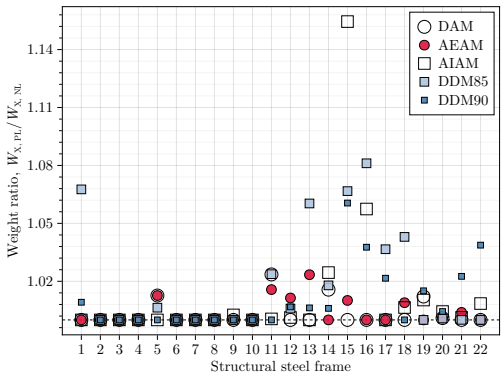

Fig. 4: Weights ratios between the optimal designs obtained using proportional and nonproportional loadings.

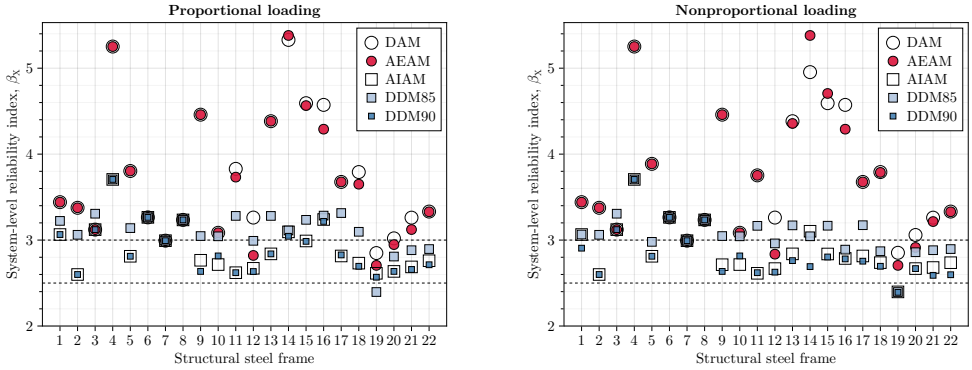

Fig. 5: System-level reliability indices of the optimal designs obtained using the design methods of interest.

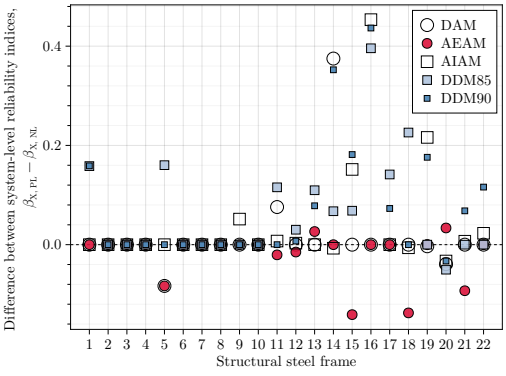

Fig. 6: Difference between the system-level reliability indices of the optimal designs obtained using the proportional and nonproportional loading.

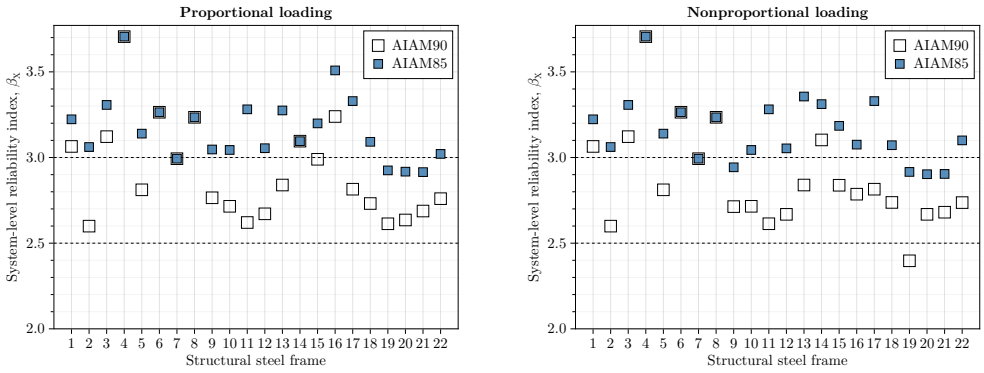

Fig. 7: System reliability indices of the optimal designs obtained using the AIAM with the reduction factors of 0.85 and 0.90.

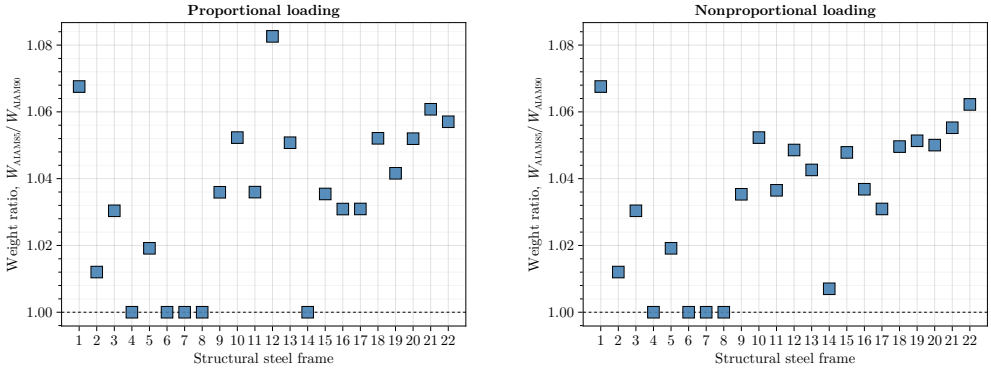

Fig. 8: Weights ratios between the optimal designs obtained using the AIAM with the reduction factors of 0.85 and 0.90.

TABLES

Table 1. Statistics of the random scaling factors.

Random scaling factor	Distribution	Mean, $\boldsymbol{\mu}$	Standard deviation, $\boldsymbol{\sigma}$
$\boldsymbol{a_1}/L$	Normal	0.000556	0.000427
$\boldsymbol{a_2}/L$	Normal	0.000139	0.000071
$\boldsymbol{a_3}/L$	Normal	0.000073	0.000078

Table 2. Statistics of the random variables associated the cross-sectional dimensions of W-shaped sections.

Dimension	Distribution	Mean, $\boldsymbol{\mu}$	Coefficient of variation, $\boldsymbol{V}$
Depth, $\boldsymbol{d}/d_n$	Normal	1.001	0.0044
Flange width, $\boldsymbol{b_{f1}}/b_{f1,n}$	Normal	1.012	0.0100
Flange width, $\boldsymbol{b_{f2}}/b_{f2,n}$	Normal	1.015	0.0095
Web thickness, $\boldsymbol{t_w}/t_{w,n}$	Normal	1.055	0.0400
Flange thickness, $\boldsymbol{t_{f1}}/t_{f1,n}$	Normal	0.988	0.0440
Flange thickness, $\boldsymbol{t_{f2}}/t_{f2,n}$	Normal	0.988	0.0490

Table 3. Correlation matrix of the random variables associated the cross-sectional dimensions of W-shaped sections.

Dimension	$\boldsymbol{d}/d_n$	$\boldsymbol{b_{f1}}/b_{f1,n}$	$\boldsymbol{b_{f2}}/b_{f2,n}$	$\boldsymbol{t_w}/t_{w,n}$	$\boldsymbol{t_{f1}}/t_{f1,n}$	$\boldsymbol{t_{f2}}/t_{f2,n}$
$\boldsymbol{d}/d_n$	1	-0.0068	+0.0534	+0.0399	-0.0686	-0.0989
$\boldsymbol{b_{f1}}/b_{f1,n}$		1	+0.6227	-0.2142	-0.2681	-0.1456
$\boldsymbol{b_{f2}}/b_{f2,n}$			1	-0.2132	-0.1596	-0.0423
$\boldsymbol{t_w}/t_{w,n}$				1	+0.2368	+0.2451

$t_{f1}/t_{f1,n}$		1	+0.7634
$t_{f2}/t_{f2,n}$	Sym.		1

Note that the original study by Melcher et al. (2004) as well as the study by Zhang et al. (2016a) erroneously report this correlation matrix with non-symmetric upper and lower triangular parts. In this study, the upper triangular part was assumed to be correct and used for further system reliability analysis.

Table 4. Weight ratios between the optimal designs obtained using the design methods of interest and the optimal designs obtained using the DAM.

Frame	Proportional loading					Nonproportional loading				
	W_{DAM} (kg)	$\frac{W_{AEAM}}{W_{DAM}}$	$\frac{W_{AIAM}}{W_{DAM}}$	$\frac{W_{DDM85}}{W_{DAM}}$	$\frac{W_{DDM90}}{W_{DAM}}$	W_{DAM} (kg)	$\frac{W_{AEAM}}{W_{DAM}}$	$\frac{W_{AIAM}}{W_{DAM}}$	$\frac{W_{DDM85}}{W_{DAM}}$	$\frac{W_{DDM90}}{W_{DAM}}$
1	1,555	1.000	0.874	0.933	0.874	1,555	1.000	0.874	0.874	0.866
2	5,898	1.000	0.890	0.901	0.890	5,898	1.000	0.890	0.901	0.890
3	956	1.000	1.000	1.030	1.000	956	1.000	1.000	1.030	1.000
4	6,144	1.000	0.786	0.786	0.786	6,144	1.000	0.786	0.786	0.786
5	2,127	1.000	0.819	0.835	0.819	2,100	1.000	0.829	0.840	0.829
6	1,911	1.000	1.000	1.000	1.000	1,911	1.000	1.000	1.000	1.000
7	1,795	1.000	1.000	1.000	1.000	1,795	1.000	1.000	1.000	1.000
8	2,339	1.000	1.000	1.000	1.000	2,339	1.000	1.000	1.000	1.000
9	14,713	1.000	0.756	0.783	0.742	14,713	1.000	0.754	0.783	0.742
10	16,286	1.000	0.769	0.810	0.776	16,286	1.000	0.769	0.810	0.776
11	5,556	0.992	0.817	0.847	0.817	5,428	1.000	0.836	0.847	0.837
12	8,365	0.993	0.739	0.794	0.737	8,365	0.982	0.738	0.789	0.732
13	15,445	1.000	0.744	0.809	0.744	15,445	0.977	0.744	0.763	0.739
14	14,898	0.993	0.717	0.691	0.679	14,668	1.008	0.711	0.689	0.685
15	15,264	0.921	0.781	0.807	0.776	15,264	0.912	0.677	0.757	0.731
16	14,075	0.960	0.784	0.827	0.793	14,075	0.960	0.742	0.765	0.764
17	23,579	1.000	0.748	0.782	0.753	23,579	1.000	0.748	0.754	0.738
18	147,507	1.004	0.817	0.846	0.810	147,507	0.995	0.812	0.811	0.810
19	173,323	0.973	0.887	0.918	0.883	171,247	0.985	0.888	0.929	0.881
20	201,085	0.986	0.857	0.889	0.857	200,891	0.986	0.855	0.889	0.855
21	169,382	0.983	0.833	0.874	0.833	169,382	0.979	0.832	0.874	0.815
22	279,319	0.990	0.849	0.885	0.841	279,319	0.990	0.842	0.885	0.810
μ		0.991	0.839	0.866	0.837		0.990	0.833	0.853	0.831
σ		0.019	0.091	0.087	0.094		0.021	0.099	0.094	0.097
V (%)		1.9	10.9	10.1	11.3		2.1	11.9	11.0	11.7
Min.		0.921	0.717	0.691	0.679		0.912	0.677	0.689	0.685
Max.		1.004	1.000	1.030	1.000		1.008	1.000	1.030	1.000

Table 5. System-level reliability indices of the optimal designs.

Frame	Proportional loading					Nonproportional loading				
	DAM	AEAM	AIAM	DDM85	DDM90	DAM	AEAM	AIAM	DDM85	DDM90
1	3.441	3.441	3.065	3.223	3.065	3.441	3.441	3.065	3.065	2.906
2	3.376	3.376	2.599	3.061	2.599	3.376	3.376	2.599	3.061	2.599
3	3.122	3.122	3.122	3.307	3.122	3.122	3.122	3.122	3.307	3.122
4	5.252	5.252	3.706	3.706	3.706	5.252	5.252	3.706	3.706	3.706
5	3.804	3.804	2.812	3.139	2.812	3.887	3.887	2.812	2.979	2.812
6	3.264	3.264	3.264	3.264	3.264	3.264	3.264	3.264	3.264	3.264
7	2.993	2.993	2.993	2.993	2.993	2.993	2.993	2.993	2.993	2.993
8	3.235	3.235	3.235	3.235	3.235	3.235	3.235	3.235	3.235	3.235
9	4.459	4.459	2.765	3.047	2.635	4.459	4.459	2.714	3.047	2.635
10	3.085	3.085	2.715	3.044	2.816	3.085	3.085	2.715	3.044	2.816
11	3.829	3.732	2.621	3.281	2.621	3.753	3.753	2.613	3.166	2.621
12	3.262	2.821	2.671	2.991	2.634	3.262	2.836	2.668	2.961	2.627
13	4.383	4.383	2.839	3.281	2.839	4.383	4.357	2.839	3.171	2.761
14	5.329	5.381	3.095	3.112	3.044	4.954	5.381	3.103	3.044	2.692
15	4.593	4.565	2.990	3.235	2.985	4.593	4.706	2.838	3.167	2.803
16	4.573	4.290	3.239	3.285	3.217	4.573	4.290	2.786	2.889	2.781

17	3.677	3.677	2.815	3.315	2.827	3.677	3.677	2.815	3.173	2.754
18	3.791	3.650	2.731	3.096	2.695	3.791	3.788	2.738	2.870	2.695
19	2.849	2.706	2.613	2.396	2.568	2.852	2.706	2.397	2.396	2.392
20	3.020	2.948	2.635	2.808	2.635	3.059	2.914	2.668	2.859	2.668
21	3.261	3.123	2.688	2.882	2.658	3.261	3.215	2.681	2.882	2.590
22	3.332	3.329	2.760	2.896	2.713	3.332	3.329	2.737	2.896	2.597
$\boldsymbol{\mu}$	3.724	3.665	2.908	3.118	2.895	3.709	3.685	2.869	3.053	2.821
$\boldsymbol{\sigma}$	0.730	0.754	0.283	0.252	0.289	0.692	0.761	0.288	0.241	0.292
$\boldsymbol{V}$ **(%)**	19.6	20.6	9.7	8.1	10.0	18.7	20.6	10.0	7.9	10.4
Min.	2.849	2.706	2.599	2.396	2.568	2.852	2.706	2.397	2.396	2.392
Max.	5.329	5.381	3.706	3.706	3.706	5.252	5.381	3.706	3.706	3.706

Table 6. Weights, weight ratios, and system-level reliability indices of the optimal designs obtained using the AIAM with the reduction factor of 0.85 on E and F_y.

Frame	**Proportional loading**			**Nonproportional loading**		
	$\boldsymbol{W_{\mathrm{AIAM85}}}$ **(kg)**	$\boldsymbol{\frac{W_{\mathrm{AIAM85}}}{W_{\mathrm{DAM}}}}$	$\boldsymbol{\beta_{\mathrm{AIAM85}}}$	$\boldsymbol{W_{\mathrm{AIAM85}}}$ **(kg)**	$\boldsymbol{\frac{W_{\mathrm{AIAM85}}}{W_{\mathrm{DAM}}}}$	$\boldsymbol{\beta_{\mathrm{AIAM85}}}$
1	1,451	0.933	3.223	1,451	0.933	3.223
2	5,311	0.901	3.061	5,311	0.901	3.061
3	985	1.030	3.307	985	1.030	3.307
4	4,831	0.786	3.706	4,831	0.786	3.706
5	1,775	0.835	3.139	1,775	0.845	3.139
6	1,911	1.000	3.264	1,911	1.000	3.264
7	1,795	1.000	2.993	1,795	1.000	2.993
8	2,339	1.000	3.235	2,339	1.000	3.235
9	11,517	0.783	3.047	11,481	0.780	2.943
10	13,184	0.810	3.044	13,184	0.810	3.044
11	4,705	0.847	3.281	4,705	0.867	3.281
12	6,696	0.800	3.054	6,477	0.774	3.053
13	12,070	0.781	3.275	11,976	0.775	3.356
14	10,681	0.717	3.095	10,498	0.716	3.312
15	12,350	0.809	3.199	10,826	0.709	3.185
16	11,382	0.809	3.508	10,826	0.769	3.075
17	18,184	0.771	3.330	18,184	0.771	3.330
18	126,778	0.859	3.092	125,673	0.852	3.072
19	160,070	0.924	2.925	159,920	0.934	2.916
20	181,389	0.902	2.917	180,275	0.897	2.903
21	149,668	0.884	2.915	148,697	0.878	2.904
22	250,650	0.897	3.021	249,762	0.894	3.100
$\boldsymbol{\mu}$		0.867	3.165		0.860	3.155
$\boldsymbol{\sigma}$		0.087	0.195		0.096	0.191
$\boldsymbol{V}$ **(%)**		10.0	6.2		11.1	6.0
Min.		0.717	2.915		0.709	2.903
Max.		1.030	3.706		1.030	3.706